AD_____

Award Number: W81XWH-04-1-0098

TITLE: Radiation Sensitization Via Inhibiting Survival of Prostate Cancer and its Vascular Endothelium

PRINCIPAL INVESTIGATOR: Bo Lu, Ph.D.

CONTRACTING ORGANIZATION: Vanderbilt University
Nashville, Tennessee 37232-2103

REPORT DATE: February 2005

TYPE OF REPORT: Annual Summary

PREPARED FOR: U.S. Army Medical Research and Materiel Command
Fort Detrick, Maryland 21702-5012

REPORT DOCUMENTATION PAGE

Form Approved
OMB No. 074-0188

1. AGENCY USE ONLY (Leave blank)	2. REPORT DATE	3. REPORT TYPE AND DATES COVERED
	February 2005	Annual Summary (1 Feb 2004 - 31 Jan 2005)

4. TITLE AND SUBTITLE
Radiation Sensitization Via Inhibiting Survival of Prostate Cancer and its Vascular Endothelium

5. FUNDING NUMBERS
W81XWH-04-1-0098

6. AUTHOR(S)
Bo Lu, Ph.D.

7. PERFORMING ORGANIZATION NAME(S) AND ADDRESS(ES)
Vanderbilt University
Nashville, Tennessee 37232-2103

E-Mail: Bo.lu@vanderbilt.edu

8. PERFORMING ORGANIZATION REPORT NUMBER

9. SPONSORING / MONITORING AGENCY NAME(S) AND ADDRESS(ES)
U.S. Army Medical Research and Materiel Command
Fort Detrick, Maryland 21702-5012

10. SPONSORING / MONITORING AGENCY REPORT NUMBER

11. SUPPLEMENTARY NOTES

12a. DISTRIBUTION / AVAILABILITY STATEMENT
Approved for Public Release; Distribution Unlimited

12b. DISTRIBUTION CODE

13. ABSTRACT (Maximum 200 Words)

We have proposed that Akt/mTOR signaling mediates cell survival and contributes to radioresistance. We intend to investigate the cellular and molecular mechanism by which inhibition of Akt/mTOR or overexpression of PTEN in both prostate cancer and its vasculature results in radiosensitization. In addition, we propose to determine possible association between level or activity of these molecules and clinical response to radiotherapy. We have found that irradiation activates Akt/mTOR signaling and combination of radiation and mTOR inhibitors enhances anti-angiogenic effects of irradiation via upregulation of apoptosis. We will investigate the interaction of Akt, Pten and mTOR and its relevance in the targeted therapeutics of prostate cancer.

14. SUBJECT TERMS	15. NUMBER OF PAGES
Prostate cancer, radiotherapy, Akt, Pten, mTOR	45
	16. PRICE CODE

17. SECURITY CLASSIFICATION OF REPORT	18. SECURITY CLASSIFICATION OF THIS PAGE	19. SECURITY CLASSIFICATION OF ABSTRACT	20. LIMITATION OF ABSTRACT
Unclassified	Unclassified	Unclassified	Unlimited

Table of Contents

1. Introduction:

We have proposed that Akt/mTOR signaling mediates cell survival and contributes to radioresistance. We intend to investigate the cellular and molecular mechanism by which inhibition of Akt/mTOR or overexpression of PTEN in both prostate cancer and its vasculature results in radiosensitization. In addition, we propose to determine possible association between level or activity of these molecules and clinical response to radiotherapy.

2. Body:

To accomplish the proposed studies: we have the following Statement of Work for the first 12 months:

Task 1. To determine whether Akt and mTOR contribute to radiation resistance in prostate cancer and its vascular endothelium (Months 1-12):

a. Determine whether Akt is required for the survival phenotype in irradiated prostate cancer and its vascular endothelium, via adenoviral transfer of dominant-negative Akt (Months 1-4): Our preliminary results showed Akt results in increased cell survival.

b. Determine whether irradiation activates mTOR signaling pathway in prostate cancer cells or endothelial cells, by Western analyses (Months 5-8): We found that irradiation activates mTOR signaling in HUVEC cells, which is mediated by PI3 kinase pathway. (Please see reference 1)

c. Determine whether inhibition of mTOR by Rapamycin enhances radiotherapy in prostate cancer cells or endothelial cells, by regulating cell survival or apoptosis (Months 9-12): We have found mTOR inhibitors such as Rapamycin and Rad001 increased apoptosis induced by irradiation in HUVEC cells. (Please see reference 1).

In addition, we have collected 100 tissue samples of prostate cancer and have established a corresponding database, which will be expanded to 500 patients in the next 12-24 months. Preliminary analyses of several genetic polymorphisms have established the feasibility of Task 4 (Please see reference 2-4).

We have also tested several novel therapeutic agents for their antiangiogenic property, which may be tested in the prostate cancer for their ability to downregulate the Akt/mTOR signaling (Please see reference 5-7).

3. Key Research Accomplishments:

mTOR inhibitors, rapamycin and Rad001, sensitize endothelial cells to radiation by decreasing cell survival:

To determine whether inhibition of mTOR sensitizes HUVEC cells to radiotherapy, clonogenic assays were performed. HUVEC cells were treated with either 100 nM of Rapamycin, 5 nM of Rad001 or a DMSO control and incubated for one hour. This was followed with escalating radiation doses from 0-7 Gy. The Rapamycin or DMSO was washed off after irradiation. After 2 weeks, colonies were stained and the scored colonies were graphed. Cells treated with rapamycin or Rad001 alone had reduced plating efficiency. Interestingly, rapamycin and Rad001 significantly lowered the survival curve of irradiated HUVEC cells as shown in Figure 1.

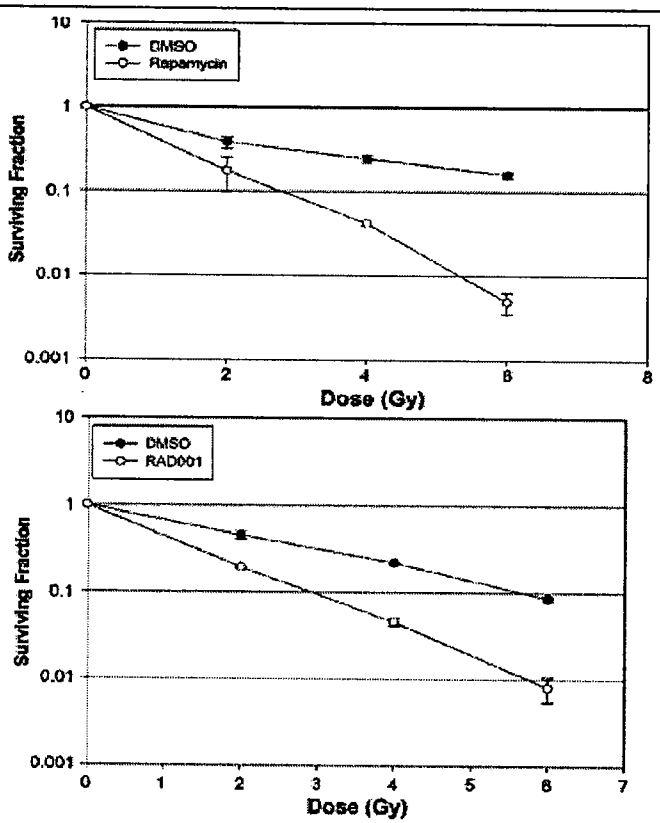

Figure 1 mTOR inhibition radiosensitizes HUVEC cells. GL261 and HUVEC were treated with 100 nM of rapamycin, 5 nM of Rad001, or DMSO for 1 h. Cells were then irradiated with indicated doses of radiation and media was changed. After 2 weeks, colonies were scored. Survival curves for HUVEC treated with radiation alone and radiation with rapamycin (100 nM) at the indicated radiation doses, and HUVEC treated with radiation alone and radiation with Rad001 (5 nM) at the indicated radiation doses are shown

Irradiation induces mTOR signaling in endothelial cells:

In order to determine whether irradiation activates the mTOR signaling pathway in endothelial cells, HUVEC cells were irradiated with 3 Gy and phosphorylated mTOR protein levels were measured by Western immunoblots which were probed for with p-mTOR antibody at the indicated time points. As shown in Figure 2A, phosphorylated mTOR was increased at 15 minutes following treatment with 3 Gy in HUVEC. The increase in phospho-mTOR persisted at one hour after irradiation, without detectable change of total mTOR protein during these time points. In order to establish whether activation of mTOR signaling was mediated by PI3 kinase, the downstream marker of mTOR signaling, phospho-S6 was determined. HUVEC cells were treated with LY294002 (3 μM), a known PI3K inhibitor or Rad001 (50 nM). 30 minutes after treatment with either inhibitor, cells were treated with 3 Gy of radiation. Cell lysates were then collected and analyzed by gel electrophoresis, using antibody for phospho-S6 and total S6 protein. As shown in Figure 2B, HUVEC treated with 3 Gy showed increased levels of S6 phosphorylation. Cells treated with LY294002 or Rad001 alone showed very little S6 phosphorylation either with or without irradiation, similar to non-irradiated HUVEC.

mTOR inhibition induces apoptosis in HUVEC:

To determine whether mTOR inhibition induces apoptosis in HUVEC we used western analysis to probe for cleaved caspase 3. HUVEC were treated with vehicle (DMSO), 3 Gy, Rad001 (50 nM) and Rad001 with 3 Gy. Cells were treated with Rad001 one hour prior to radiation and proteins were collected 6 hours later. Cleaved caspase 3 and total caspase 3 were probed for as

shown in Figure 2C. DMSO alone showed no induction of caspase 3 cleavage, whereas there was minor induction of caspase 3 cleavage in cells treated with 3 Gy or Rad001 alone. However, combined therapy with Rad001 and 3 Gy resulted in the greatest increase in Caspase 3 cleavage when compared with the other groups. Total caspase 3 showed no change in all groups.

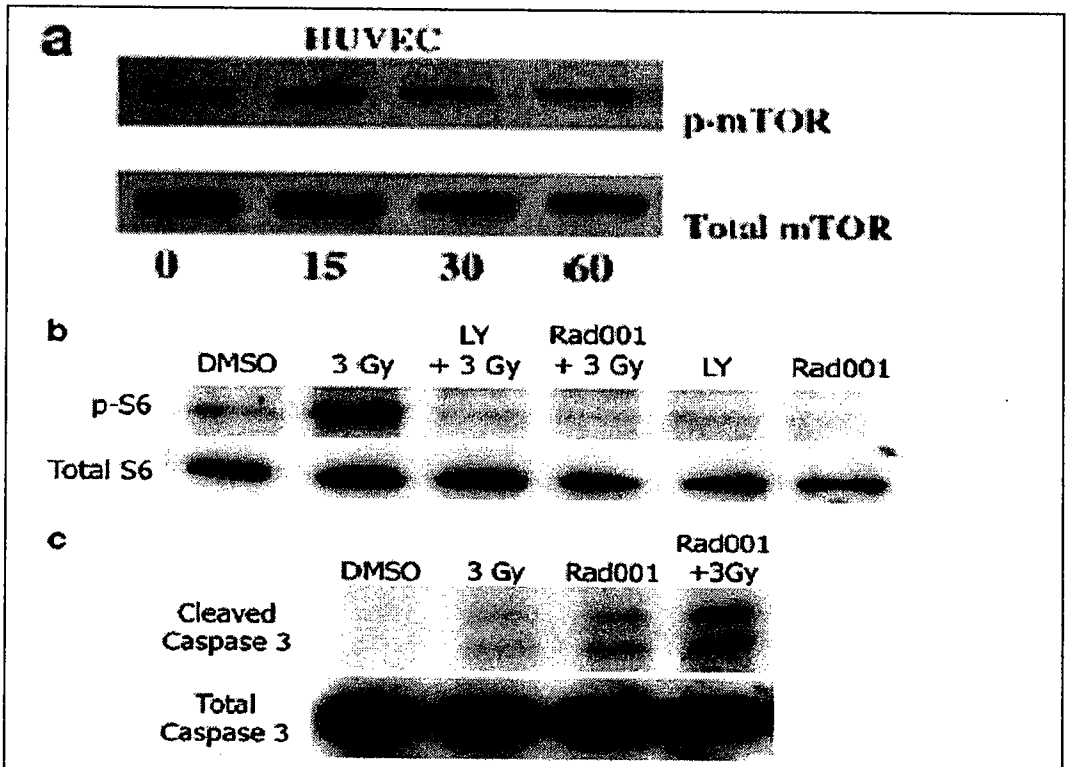

Figure 2 Radiation induces mTOR phosphorylation in HUVEC: HUVEC were treated with 3Gy and cell lysates were collected at 0, 15, 30, and 60 min. HUVEC lysates probed with phospho-mTOR and total mTOR antibodies at the indicated time points. (a) are shown. HUVEC were treated with DMSO, 3 Gy, LY294002 (3 mM), Rad001 (50 nM), LY294002 with 3 Gy, and Rad001 with 3 Gy. Western blot probed for phosphorylated S6 and total S6 (b) are shown. HUVEC were treated with DMSO, 3 Gy, Rad001 (50 nM) or Rad001 with 3 Gy. Western blots probed for cleaved caspase 3 and total caspase 3 (c) are shown.

Rapamycin sensitizes vascular endothelium to radiation injury:

Since rapamycin reduced the survival of HUVEC cells, we studied rapamycin effects on tumor angiogenesis. HUVEC cells were treated with either 100 nM rapamycin or DMSO for one hour. Cells were then irradiated with 0 or 3Gy. Rapamycin and DMSO were washed off after irradiation. The endothelial cell morphogenesis assay was performed to examine the ability of the treated HUVECs to produce tubular structures *in vitro*. As shown in Figure 3, HUVEC cells that were treated with both rapamycin and 3 Gy formed 3-4 fold less tubular structures, in contrast to the DMSO group. The groups treated with radiotherapy or rapamycin alone had nearly a one fold reduction of tubular structure.

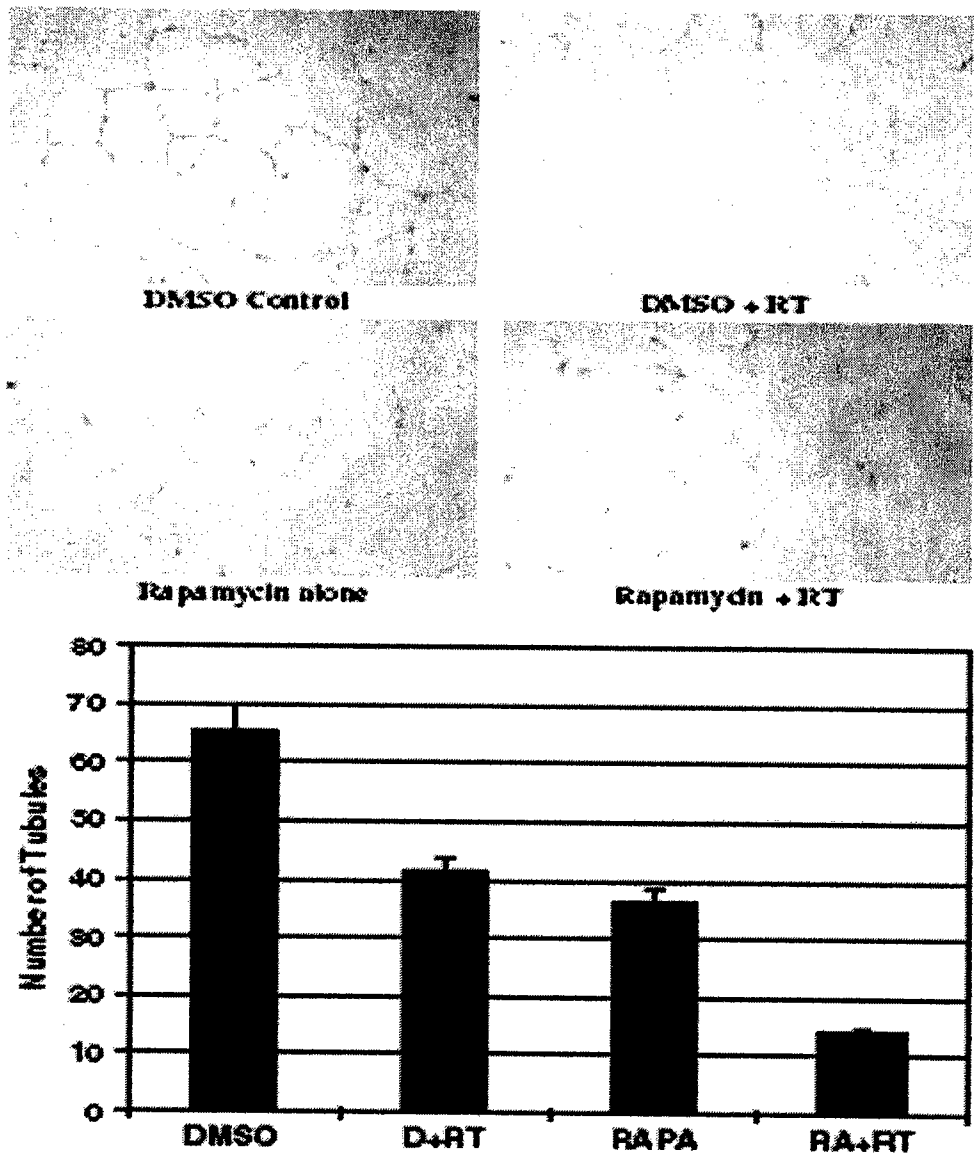

Figure 3 Rapamycin sensitizes vascular endothelium to radiation injury: HUVEC (4.8_104 cells) were treated with rapamycin (100 nM), radiation, or both. They were then resuspended and plated on 24-well plates coated with Matrigel. After 24 h, the media were gently aspirated and the cells were fixed and stained. The slides were examined for tube formation by microscopy. Representative figures and quantification of tubular structures are shown. Data are shown as the mean7s.d. DMSO-treated HUVEC had an average of 65 tubes per high powered field (s.d.¼4.97), HUVEC treated with DMSO and 3Gy had 41.5 tubes (s.d.½2.65), HUVEC treated with rapamycin alone had 36.5 (s.d.½2.38), and HUVEC treated with rapamycin and 3Gy had 14.25 (s.d.¼0.96)

Rad001, selectively sensitize prostate cancer cells to radiation by decreasing cell survival:

To determine whether inhibition of mTOR sensitizes HUVEC cells to radiotherapy, clonogenic assays were performed. PC3 prostate cancer cells were treated with either 5nM or 10nM of Rad001 or a DMSO control and incubated for one hour. This was followed with escalating radiation doses from 0-5 Gy. The Rapamycin or DMSO was washed off after irradiation. After 2 weeks, colonies were stained and the scored colonies were graphed. Cells treated with Rad001 alone had reduced plating efficiency. Interestingly, Rad001 significantly lowered the survival curve of irradiated PC3 cells as shown in Figure 4.

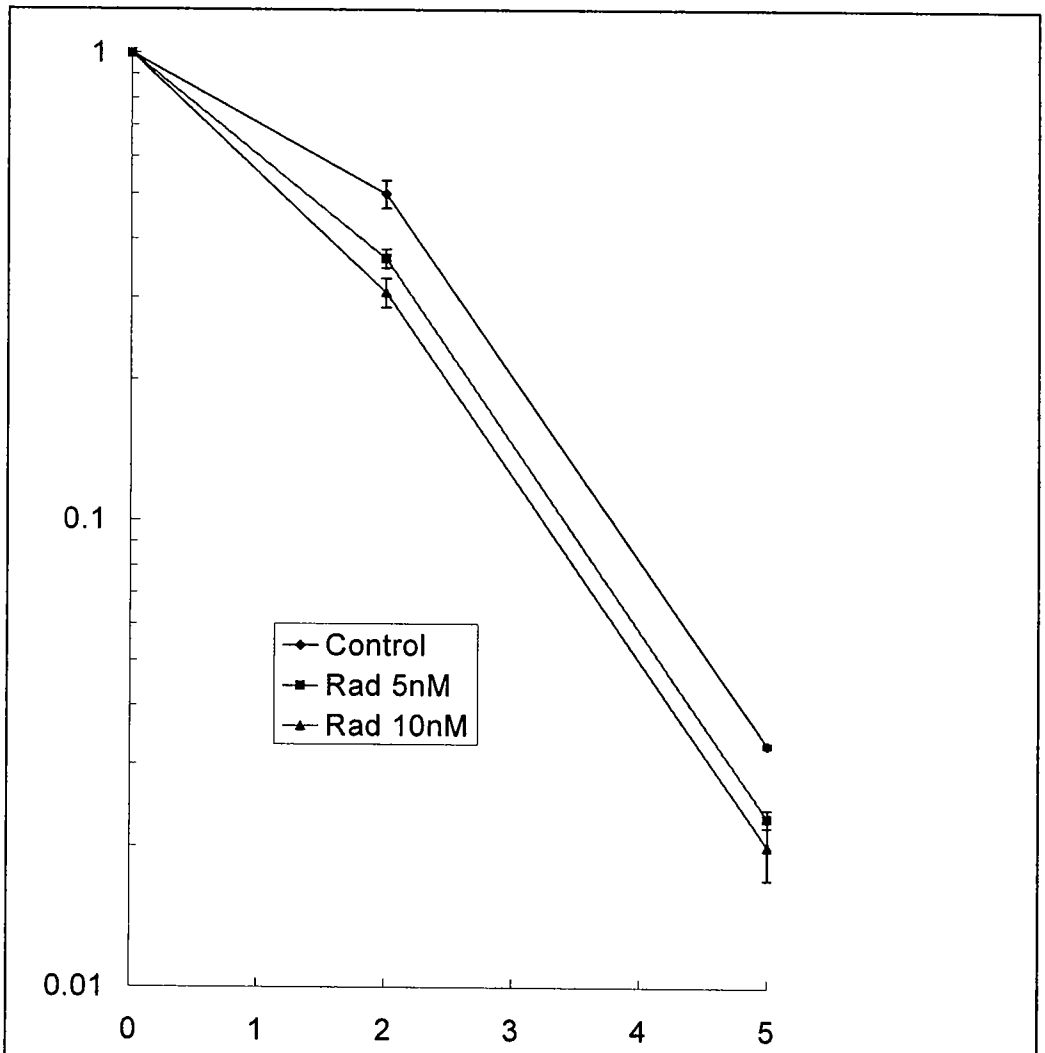

Figure 4. mTOR inhibition radiosensitizes prostate cancer cells. PC3 cells were treated with 5nM or 10 nM of Rad001, or DMSO for 1 h. Cells were then irradiated with indicated doses of radiation and media was changed. After 2 weeks, colonies were scored. Survival curves for HUVEC treated with radiation alone and radiation with Rad001 at the indicated radiation doses are shown.

Establishing clinical database:
We found 98 Caucasian patients with prostate cancer who underwent prostatectomy at Vanderbilt Hospital in 1997. The study was approved by Institutional Review Board (IRB# 030986) at Vanderbilt University School of Medicine. All patients had clinically localized prostate cancer and were treated with radical prostatectomy as a primary treatment. All patients had adenocarcinoma confirmed histologically. The patients were followed at Vanderbilt Hospital or at local hospitals with a mean follow-up of 62 months. Patients` age ranged 40 to 81 with a median age of 63 years. All pathological information was reviewed by one pathologist and the tumor differentiation was evaluated using Gleason`s score criteria. Clinical stage was classified according to the AJCC TNM staging system. The Clinical and histological characteristics of the patients are summarized in Table 1.

Table 1
Associations of endostatin polymorphisms with other clinical and pathological parameters

Factors	4349 polymorphism		*P* value
	4349G/G(104D/D) n(%)	4349G/A(104D/N) n(%)	
Age (y)			
⩽60	30(88.24)	4(11.76)	0.6886
60–70	42(80.77)	10(19.23)	
>70	10(83.33)	2(16.67)	
PSA			
⩽4	12(70.59)	5(29.41)	0.2791
4–10	45(86.54)	7(13.46)	
>10	25(86.21)	4(13.79)	
Gleason grade			
⩽6	54(87.10)	8(12.90)	0.2640
> 6	28(77.78)	8(22.22)	
Clinical stage			
I	7(77.78)	2(22.22)	0.7479
II	57(85.07)	10(14.93)	
III	18(81.82)	4(18.18)	

Tissue preparation and DNA extraction
Using a standard microtome with disposable blades, 5um thickness sections of a representative areas of normal prostatic glands were cut from the paraffin embedded blocks and stained with Hematoxylin and eosin(H&E) and then examined under a microscope to verify the absence of prostate cancer. 5um thickness section (about 1ug) from each patient was used for DNA extraction. The sections were deparaffinized with xylene at room temperature for 30minutes twice. Then the deparaffinized tissue was washed with 100% ethanol twice. After the ethanol had evaporated completely, the tissue was completely lysed with proteinase K. Then QIAamp DNA Mini Kit(QIAGEN Inc, Valencia, CA) was used to extract and purify DNA from the tissues according to the tissue protocol of the kit.

Polymorphism Genotyping
The allelic discrimination of the *E-cadherin* gene -160 C→A and -347 G→GA polymorphisms were assessed with the ABI PRISM 7900HT Sequence Detection System(Applied Biosystems). PCR was performed with a total volume of 5ul, which contained approximately 2.5ng DNA,1×Taqman Universal PCR Master Mix, each primer at a concentration of 900nM, and each probe at a concentration of 200nM. Taqman probes for -160 polymorphism were: A allele specific: 5`-VIC- CTA GCA ACT CCA GGC TAG AGG GTC AAC GCG TCT ATG CGA GGC CGG GTG GGC -NFQ-3`; C-allele specific: 5`-FAM- CTA GCA ACT CCA GGC TAG

AGG GTC ACC GCG TCT ATG CGA GGC CGG GTG GGC -NFQ-3`. Primers of -160 polymorphism were obtained from Applied Biosystems (Assay ID: C_11934298_10). Taqman probes for -347 polymorphism were: G allele specific: 5`-FAM- AAA GAG TGA GCC CCA TC-NFQ-3`; A-allele specific: 5`-VIC- AAA GAG TGA GAC CCC ATC-NFQ-3`. Forward primer for -347 polymorphism sequence was: 5` -CAC CAC TGC ACT CCA GCT T-3` and reverse primer sequence was: 5`-GCT GAG TTC TTT TGT TTT GGG ATT T-3`. The thermal cycling conditions were as follows: 95^0C for 10min to activate the AmpliTaq Gold enzyme, followed by 40 cycles of 15 seconds at 95^0C and 60 seconds at 60^0C. The fluorescence levels were measured with an ABI PRISM 7900HT Sequence Detector(Applied Biosystems), resulting in clear identification of three genotypes of each polymorphism.
The laboratory staff was blind to the identity of the subjects. Quality control(QC) samples were included in the genotyping assays. Each 384 well plate contained four water, eight CEPH 1347-02 DNA, eight blinded QC samples, and eight unblinded QC samples. The blinded and unblinded QC samples were taken from the second tube of study samples included in this study.

E-cadherin polymorphisms genotyping

With Taqman single nucleotide polymorphism(SNP) genotyping assay, *E-cadherin* polymorphism genotypes of DNA from the 98 tissues were successfully detected with a quality control agreement rate of 100%. The frequencies of *E-cadherin* -160 polymorphism genotypes were 47.96%(47/98) for -160C/C, 43.88%(43/98) for -160C/A, and 8.16%(8/98) for -160A/A. *E-cadherin* -347 polymorphism genotypes were G/G:68.37%(67/98), -347G/GA: 27.55%(27/98) and -347GA/GA: 4.08%(4/98) respectively. The distribution of the genotypes of the -160C/A and -347G/GA polymorphism in this group of patients did not differ significantly from those predicted by the Hardy-Weinberg distribution (for -160C→A: X^2=0.398, P=0.5281, for -347G→GA: X^2=0.363, P=0.5468).

The association of E-cadherin polymorphisms with other clinical and pathological parameters

Using the Chi-square test, we found that *E-cadherin* -160 polymorphism genotype had no association with patients` age, prostate-specific antigen(PSA) level, Gleason grade and clinical stage (p>0.05, see Table 1); Chi-square analysis of the -340 polymorphism genotypes also showed no association with these variables (p>0.05, see Table 1). In combination analysis(Patients were divided into two subgroups: those with -160C/C and -347G/G and those with other genotypes), there was no significant association between -160C/-347G homozygosities (with both -160C/C and -347G/G) and patients` age, PSA level, Gleason grade and clinical stage either (p>0.05) (Table1).

Survival analysis

The Kaplan-Meier method was used to compute survival rates and the log-rank test was applied to test the difference in survival across different genotypes. 5-year relapse free survival(RFS) rates and overall survival(OS) rates for this group of patients were 87.71% and 95.64% respectively. There was no significant difference between subjects with -160C/C and those with other genotypes(-160A/A or -160C/A) in RFS and OS (Log-rank test, P=0.0764 and 0.2746 respectively) (Figure1A,B); there was no significant difference between subjects with -347G/G and those with other genotypes(-347GA/GA or -347GA/A) in RFS and OS (Log-rank test, P=0.9416 and 0.7367 respectively) (Figure1C,D). In the combination analysis, the difference in RFS or OS between patients with -160C/-347G homozygosities(both -160C/C and -347G/G) and those with other genotypes was not significant either(Log-rank test, P=0.1418 and 0.2434 respectively) (Figure1E,F)

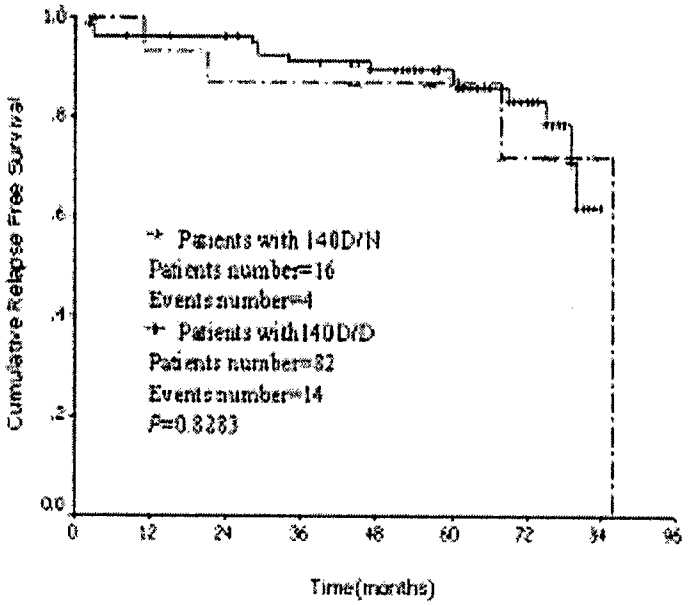

(A)

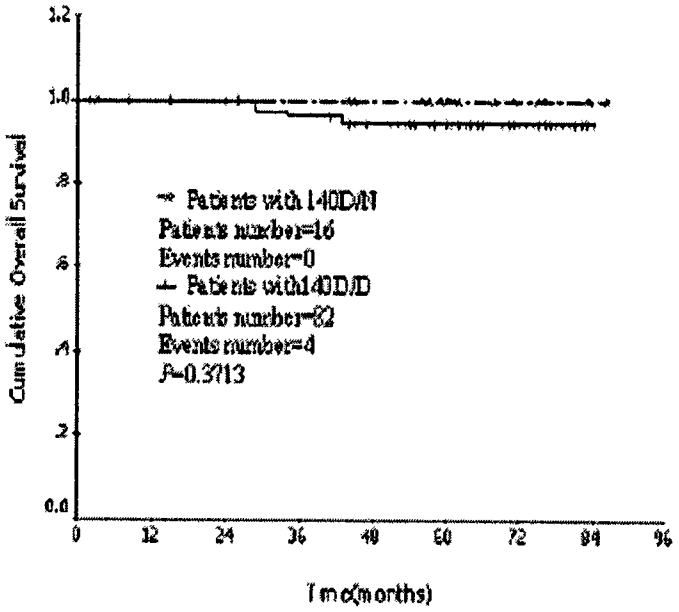

(B)

Fig. 1. Relapse free survival and overall survival curves. (A) RFS curves for patients with 4349G/G(140D/D) genotype and those with 4349G/A(140D/N); (B) OS curves for patients with 4349G/G(140D/D) genotype and those with 4349G/G (140D/N).

4. Reportable outcomes:

1. Eric Shinohara, Kenneth Niermann, Carolyn Cao, Fenghua Zeng, Dennis E. Hallahan, and Bo Lu. mTOR inhibitors as a potential anti-angiogenesis agent enhanced efficacy of radiotherapy. 2005 May 23; [Epub ahead of print]

2. Li HC, Eric Shinohara and Bo Lu. Endostatin polymorphism 4349G/A(D104N) is not Associated with Aggressiveness of Disease in Prostate Cancer *Dis Markers* Volume 21, Number 1, 2005

3. Li HC, Eric T Shinohara and Bo Lu Plasminogen activator inhibitor-1(PAI-1) promoter polymorphism is not associated with prognosis in prostate cancer (accepted, *Clinical Oncology*).

4. Tissue collection and database of prostate cancer.

5. Conclusions: We have found that irradiation activates Akt/mTOR signaling and combination of radiation and mTOR inhibitors enhances anti-angiogenic effects of irradiation. We will investigate the interaction of Akt, Pten and mTOR and its relevance in the targeted therapeutics of prostate cancer.

6. References:

1. Eric Shinohara , Kenneth Niermann, Carolyn Cao, Fenghua Zeng, Dennis E. Hallahan, and Bo Lu. mTOR inhibitors as a potential anti-angiogenesis agent enhanced efficacy of radiotherapy. Oncogene 2005 24: 5414-5422

2. Li HC, Eric Shinohara and Bo Lu. Endostatin polymorphism 4349G/A(D104N) is not Associated with Aggressiveness of Disease in Prostate Cancer *Dis Markers* Volume 21, Number 1, 2005

3. Li HC, Eric T. Shinohara and Bo Lu. E-cadherin promoter polymorphisms are not associated with the aggressiveness of prostate cancer in Caucasian patients. (submitted to *Int J Cancer*).

4. Li HC, Eric T Shinohara and Bo Lu Plasminogen activator inhibitor-1(PAI-1) promoter polymorphism is not associated with prognosis in prostate cancer (accepted, Clinical Oncology).

5. Carolyn Cao, Mu Yi, Dennis E. Hallahan, Bo Lu. Radiation sensitization of lung cancer through inhibition of survivin and XIAP. Oncogene. 2004 Sep 16;23(42):7047-52.

6. Carolyn Cao, Eric Shinohara, Kenneth Niermann, Dennis Hallahan, and Bo Lu. MDM2 as a radiosensitizing target for lung cancer and its vasculature. Mol Cancer Ther 2005 4: 1137-1145.

7. Carolyn Cao, Kenneth Niermann and Bo Lu. Radiation sensitization of lung cancer and its angiogenesis through inhibition of Clusterin (in print, Int J Radiat Oncol Biol Phys.).

Disease Markers 18 (2003,2004) 1–5
IOS Press

Endostatin polymorphism 4349G/A(D104N) is not associated with aggressiveness of disease in postate cancer[1]

Hecheng Li[a,**], Qiuyin Cai[b], Eric T Shinohara[c], Hui Cai[b], Carolyn Cao[c], Zuofei Wang[c], Ming Teng[c], Wei Zheng[b] and Bo Lu[c,*]
[a]*Department of Breast Surgery, Cancer Hospital/Cancer Institute, Fudan University, Shanghai, 200032, P.R. China*
[b]*Department of Medicine and Vanderbilt-Ingram Cancer Center, Vanderbilt University School of Medicine, Nashville, TN 37232, USA*
[c]*Department of Radiation Oncology and Vanderbilt-Ingram Cancer Center, Vanderbilt University School of Medicine, Nashville, TN 37232, USA*

Abstract. Endostatin is an important inhibitory molecule which mediates the sequential steps involved in angiogenesis. Lower level or impaired function of endostatin is associated with a higher risk of developing malignant solid tumors and with a worse prognosis of the disease. The *endostatin* N104 polymorphism might be associated with an impaired ability to inhibit angiogenesis. We analyzed the tissues from 98 Caucasian prostate cancer patients for the presence of D104N polymorphism. The frequencies of homozygous 4349G/G(104D/D), and heterozygous 4349G/A(104D/N) were 83.67%(82/98) and 16.33%(16/98), respectively; no individuals were homozygous 4349A/A(104N/N). With the Fisher's exact test we found the genotype of D104N was not significantly related to age, tumor grade, PSA and clinical stage ($P > 0.05$). There was no difference in relapse free survival(RFS) or overall survival(OS) between patients with 104D/N and those with 104D/D ($P = 0.8283$, 0.3713 respectively). We concluded that *endostatin* polymorphism was not associated with the aggressiveness of prostate cancer in Caucasian patients.

Keywords: Prostate cancer, endostatin, polymorphism

1. Introduction

The latest estimates of global cancer incidence show that prostate cancer has become the third most common cancer in men, with half a million new cases each year, almost 10% of all cancers in male [1–4]. Prostate cancer is usually regarded as a slow-growing tumor, and only 2.9% actually will die of the disease [5]. In order to better design therapeutic strategies for individual cases and identifying patients who would benefit from more vigilant surveillance, it would be of interest to study markers which can predict the outcome of disease. Angiogenesis, or the formation of new blood vessels from preexisting endothelium, is a fundamental step in tumor progression and metastasis [6,7]. Endostatin, a Mr 20,000 cleavage product of the COOH-terminal domain of collagen XVIII(NC1), has been considered as an important inhibitory molecules that can medicate the sequential steps involved in angiogenesis. Higher serum levels of endostatin induced experimentally in mice and rats seem to cause regression of various types of solid tumors, including prostate cancer [8–10]. In addition, Down's syndrome patients, who have a higher serum levels of endostatin because of their three copies of the

*Address for correspondence: Bo Lu, M.D., Ph.D., Department of Radiation Oncology and Vanderbilt-Ingram Cancer Center, Vanderbilt University School of Medicine, Nashville, TN 37232, USA. Fax.: +1 615 343 0161; E-mail: Bo.Lu@vanderbilt.edu.
**Visiting research fellow at Vanderbilt University School of Medicine, Nashville, TN 37232, USA.
[1]This work is supported in part by DOD PC031161(BL), RO1CA90899(WZ) and UICC fellowship ICRETT1025(HL).

ISSN 0278-0240/03,04/$17.00

Table 1
Associations of endostatin polymorphisms with other clinical and pathological parameters

Factors	4349 polymorphism		*P* value
	4349G/G(104D/D) n(%)	4349G/A(104D/N) n(%)	
Age (y)			
⩽60	30(88.24)	4(11.76)	0.6886
60–70	42(80.77)	10(19.23)	
>70	10(83.33)	2(16.67)	
PSA			
⩽4	12(70.59)	5(29.41)	0.2791
4–10	45(86.54)	7(13.46)	
>10	25(86.21)	4(13.79)	
Gleason grade			
⩽6	54(87.10)	8(12.90)	0.2640
> 6	28(77.78)	8(22.22)	
Clinical stage			
I	7(77.78)	2(22.22)	0.7479
II	57(85.07)	10(14.93)	
III	18(81.82)	4(18.18)	

COL18A1 gene, have a decreased incidence of solid tumors, including prostate cancer [11]. Thus, lower levels or an impaired function of endostatin might be associated with a higher risk of developing malignant solid tumor or with a worse prognosis of the disease. Visakorpi et al. conducted a systematic analysis of the COL18A1 gene and found a missense mutation of D104N located in the COOH-terminal globular domain NC1 of collagen XVIII, the encoding region of *endostatin* [12]. Iughetti et al. found that heterozygous N104 individuals have a higher chance of developing prostate cancer compared with homozygous D104 subjects and proposed the presence of N104 impairs the function of endostatin [13]. In the present study we hypothesize that N104 may impair the function of endostatin and in turn affect the aggressiveness of prostate cancer. To testify our hypothesis we assessed the *endostatin* polymorphism present in 98 Caucasian patients with prostate cancer to determine whether D104N is correlated with well known prognostic factors as well as relapse free survival(RFS) and overall survival(OS).

2. Materials and methods

2.1. Patient population and clinical data

The study population consisted of 98 Caucasian patients with prostate cancer who underwent prostatectomy at Vanderbilt Hospital in 1997. The study was approved by Institutional Review Board (IRB# 030986) at Vanderbilt University School of Medicine. All patients had clinically localized prostate cancer and were treated with radical prostatectomy as a primary treatment. All patients had adenocarcinoma confirmed histologically. The patients were followed at Vanderbilt Hospital or at local hospitals with a mean follow-up of 62 months. Patients' age ranged 40 to 81 with a median age of 63 years. All pathological information was reviewed by one pathologist and the tumor differentiation was evaluated using Gleason's score criteria. Clinical stage was classified according to the AJCC TNM staging system [14]. The Clinical and histological characteristics of the patients are summarized in Table 1.

2.2. Tissue preparation and DNA extraction

Using a standard microtome with disposable blades, 5 um thickness sections of a representative areas of normal prostatic glands were cut from the paraffin embedded blocks and stained with Hematoxylin and eosin (H&E) and then examined under a microscope to verify the absence of prostate cancer. 5 um thickness section (about 1 ug) from each patient was used for DNA extraction. The sections were deparaffinized with xylene at room temperature for 30 minutes twice. Then the deparaffinized tissue was washed with 100% ethanol twice. After the ethanol had evaporated completely, the tissue was completely lysed with proteinase K. Then QIAamp DNA Mini Kit (QIAGEN Inc, Valencia, CA) was used to extract extraction and purify DNA from the tissues according to the tissue protocol of the kit.

3. Polymorphism genotyping

The allelic discrimination of the *endostatin* gene 4349G/A polymorphism was assessed with the ABI

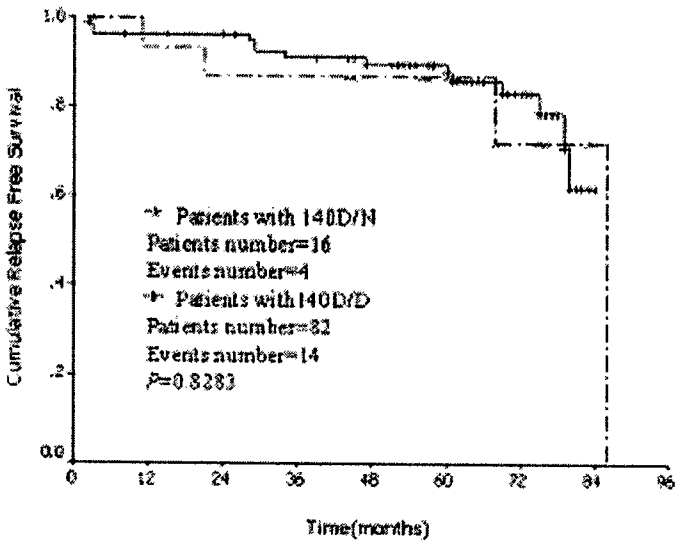

(A)

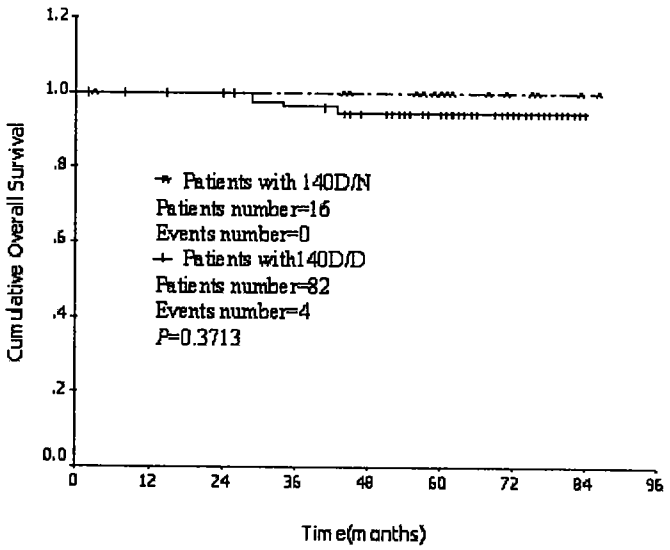

(B)

Fig. 1. Relapse free survival and overall survival curves. (A) RFS curves for patients with 4349G/G(140D/D) genotype and those with 4349G/A(140D/N); (B) OS curves for patients with 4349G/G(140D/D) genotype and those with 4349G/G (140D/N).

PRISM 7900 HT Sequence Detection System (Applied Biosystems). PCR was performed with a total volume of 5 ul, which contained approximately 2.5 ng DNA, 1 × Taqman Universal PCR Master Mix, each primer at a concentration of 900 nM, and each probe at a concentration of 200 nM. Primers for *endostatin* were from Applied Biosystems (Assay ID: C_11872896_10). Taqman probes were: A allele specific: 5′-VIC-GCC CGG GGC ACG CAT CTT CTC CTT TAA CGG CAA GGA CGT CCT GAG GCA CCC -NFQ-3′ G-allele specific:

5′-FAM- GCC CGG GGC ACG CAT CTT CTC CTT TGA CGG CAA GGA CGT CCT GAG GCA CCC -NFQ-3′. The thermal cycling conditions were as follows: 95°C for 10 min to activate the AmpliTaq Gold enzyme, followed by 40 cycles of 15 seconds at 95 °C and 60 seconds at 60°C. The fluorescence levels were measured with an ABI PRISM 7900 HT Sequence Detector (Applied Biosystems, Foster City, CA), resulting in clear identification of three genotypes of each polymorphism.

The laboratory staff was blind to the identity of the subjects. Quality control (QC) samples were included in the genotyping assays. Each 384 well plate contained four water, eight CEPH 1347-02 DNA, eight blinded QC samples, and eight unblinded QC samples. The blinded and unblinded QC samples were taken from the second tube of study samples included in this study.

4. Statistical analysis

Relapses free survival (RFS) was defined as the time between the date of the primary surgery to the date of relapse or the date of last follow-up. Overall survival (OS) was defined as time between the date of the primary surgery to the date of death or the date of last follow-up. The Kaplan-Meier method was used to compute 5-year survival rates and log-rank test was applied to test the difference in survival across different genotype. The associations between the *endostatin* polymorphism and other clinical and pathological characters was analyzed by Fisher's exact test. P-values $<$ 0.05 were considered statistically significant. All statistical analyses were two sided. We conducted the statistical analysis with SAS 9.1 *SAS* Institute Inc., Cary, NC.

5. Results

5.1. The correlation of 104D/N polymorphism with other clinical and pathological parameters

With Taqman SNP genotyping assay, the concordance of the blinded samples was 100%. Genotypes for 4349G/A polymorphism were successfully determined in 98 samples. The frequencies of homozygous 4349G(104D/D), and heterozygous 4349G/A(104D/N) were 83.67%(82/98) and 16.33%(16/98), respectively. With Fisher's exact test, *Endostatin* polymorphism was found to have no significant relationship with age (P = 0.6886), PSA (P = 0.2791), Gleason's grade (P = 0.2640) and clinical stage (P = 0.7479) (Table 1).

5.2. Survival analysis

The Kaplan-Meier method was used to compute survival rates and the log-rank test was applied to test the difference in survival across different genotypes. 5-year relapse free survival rates and overall survival rates for this group of patients were 87.71% and 95.64% respectively. There was no significant difference between subjects with D104N and those with D104D in RFS and OS (Log-rank test, P = 0.8283 and 0.3713 respectively) (Fig. 1A,B).

6. Discussion

In the current study, we analyzed the 4349G/A (D104N) polymorphism in 98 Caucasian patients and did not find any association between the polymorphism and other clinical and pathological variables, and we did not find any significant association between 4349G/A(D104N) polymorphism and patients' survival (RFS and OS) either.

Higher serum levels of endostatin induced experimentally in mice and rats seem to cause regression of various types of solid tumors, including prostate cancer [8–10]. Clinical study also showed that individuals with higher levels of endostatin might be less prone to develop solid tumors [15]. The missense mutation of D104N located in the COOH-terminal globular domain NC1 of collagen XVIII was found to be in the encoding region of *endostatin* by Visakorpi et al. in 1999 [12]. It has been recently shown that gene polymorphisms affect cancer cell proliferation, differentiation as well as tumor invasion/metastasis [16]. The possible association of D104N with cancer risk and prognosis remains poorly investigated. Iughetti et al reported that individuals heterozygous for N104 have a 2.5 times greater chance of developing prostate cancer as compared with homozygous D104 subjects (OR: 2.4, 95%CI:1.4–4.16); the author proposed that *endostatin* N104 has a decreased affinity for binding to other molecules and an impaired ability to inhibit angiogenesis [13]. In a case-control study containing 58 multiple myeloma patients, Ortega et al reported that the genotype frequencies were in Hardy-Weinberg equilibrium and that the D104N polymorphism was an unimportant determinant in multiple myeloma patients [17]. Liu et al. reported a case control study including 274 patients with leukemia and 178 normal controls. In Liu's study there were no patients homozygous for 4349A which was similar to our study; they found no association with

endostatin polymorphism and the risk of leukemia [17, 18]. Most of the previous studies showed there were no association between the D104N polymorphism and malignancies. Only Iughetti et al. reported a higher risk ratio of developing prostate cancer for heterozygous N104 individuals, but even in this study they did not find any association between the presence of the mutation and Gleason score or age at diagnosis. We not only further confirm D104N polymorphism had no relationship with Gleason score or age at diagnosis, but also demonstrate that the D104N polymorphism has no relationship with PSA level, clinical stage as well as RFS and OS of patients.

The discrepancies between our study and previous studies might due to several reasons. The translation of results from different studies might be limited due to the limited sample size and different patient selection. In our study we selected stage I or II Caucasian patients. Another reason is that we analyze the relationship between the *endostatin* polymorphism and prostate cancer from the aspect of aggressiveness of disease but not cancer risk and this will also cause the discrepancies between our study and previous ones. Last but not the least reason, most of the previous studies as well as ours were retrospective and the conclusions must be drawn cautiously. So far, to the authors' knowledge there is no data from prospective randomized study available.

In conclusion, our study indicated that the *endostatin* polymorphism 4349G/A(D104N) is not associated with aggressiveness of disease in Caucasian patients with prostate cancer.

Acknowledgments

This study was supported in part by DOD PC031161 (BL), RO1CA90889(WZ) and UICC fellowship ICRETT1025(HL). We are grateful to Regina Courtney (Department of Medicine and Vanderbilt-Ingram Cancer Center, Vanderbilt University School of Medicine, Nashville, TN 37232, USA) for her technique support in Taqman SNP genotyping assay.

References

[1] D. Parkin, Royal College of Nursing, *Momentum, Nurs Stand* **452** (1986), 1–4.

[2] D.M. Parkin, E. Laara and C.S. Muir, Estimates of the worldwide frequency of sixteen major cancers in 1980, *Int J Cancer* **41** (1988), 184–197.

[3] D.M. Parkin, P. Pisani and J. Ferlay, Estimates of the worldwide incidence of 25 major cancers in 1990, *Int J Cancer* **80** (1999), 827–841.

[4] M. Quinn and P. Babb, Patterns and trends in prostate cancer incidence, survival, prevalence and mortality, Part I: international comparisons, *BJU Int* **90** (2002), 162–173.

[5] J.A. Siegal, E. Yu and M.K. Brawer, Topography of neovascularity in human prostate carcinoma, *Cancer* **75** (1995), 2545–2551.

[6] D. Hanahan and J. Folkman, Patterns and emerging mechanisms of the angiogenic switch during tumorigenesis, *Cell* **86** (1996), 353–364.

[7] T. Sasaki, N. Fukai, K. Mann, W. Gohring, B.R. Olsen and R. Timpl, Structure, function and tissue forms of the C-terminal globular domain of collagen XVIII containing the angiogenesis inhibitor endostatin, *Embo J* **17** (1998), 4249–4256.

[8] Y. Yokoyama, J.E. Green, V.P. Sukhatme and S. Ramakrishnan, Effect of endostatin on spontaneous tumorigenesis of mammary adenocarcinoma in a transgenic mouse model, *Cancer Res* **60** (2000), 4362–4365.

[9] S.S. Yoon, H. Eto, C.M. Lin, H. Nakamura, T.M. Pawlik, S.U. Song and K.K. Tanabe, Mouse endostatin inhibits the formation of lung and liver metastases, *Cancer Res* **59** (1999), 6251–6256.

[10] G. Perletti, P. Concari, R. Giardini, E. Marras, F. Piccinini, J. Folkman and L. Chen, Antitumor activity of endostatin against carcinogen-induced rat primary mammary tumors, *Cancer Res* **60** (2000), 1793–1796.

[11] H. Hasle, I.H. Clemmensen and M. Mikkelsen, Risks of leukaemia and solid tumours in individuals with Down's syndrome, *Lancet* **355** (2000), 165–169.

[12] T. Visakorpi, Molecular genetics of prostate cancer, *Ann Chir Gynaecol* **88** (1999), 11–16.

[13] P. Iughetti, O. Suzuki, P.H. Godoi, V.A. Alves, A.L. Sertie, T. Zorick, F. Soares, A. Camargo, E.S. Moreira, C. di Loreto, C.A. Moreira-Filho, A. Simpson, G. Oliva and M.R. Passos-Bueno, A polymorphism in endostatin, an angiogenesis inhibitor, predisposes for the development of prostatic adenocarcinoma, *Cancer Res* **61** (2001), 7375–7378.

[14] Prostate, in: *American Joint Commitee on Cancer: AJCC Cancer Staging Manual*, 6 eds, Springer, New York, 2002, pp. 309–316.

[15] O. Musso, M. Rehn, N. Theret, B. Turlin, P. Bioulac-Sage, D. Lotrian, J.P. Campion, T. Pihlajaniemi and B. Clement, Tumor progression is associated with a significant decrease in the expression of the endostatin precursor collagen XVIII in human hepatocellular carcinomas, *Cancer Res* **61** (2001), 45–49.

[16] A. Loktionov, Common gene polymorphisms, cancer progression and prognosis, *Cancer Lett* **208** (2004), 1–33.

[17] M.M. Ortega, H. Nascimento, F.F. Costa, M.T. Teori and C.S. Lima, A polymorphism in the angiogenesis inhibitor, endostatin, in multiple myeloma, *Leuk Res* **27** (2003), 93–94.

[18] T.C. Liu, C.T. Peng, S.F. Lin, C.S. Chang, T.P. Chen and J.G. Chang, Assocation of endostatin D104N with leukemia, *Kaohsiung J Med Sci* **19** (2003), 1–5.

Enhanced Radiation Damage of Tumor Vasculature by mTOR Inhibitors

Eric Shinohara, Carolyn Cao, Ken Niermann, Yi Mu, Fenghua Zeng, Dennis E. Hallahan and Bo Lu[1]

Department of Radiation Oncology, Vanderbilt Ingram Cancer Center, Vanderbilt University School of Medicine, Nashville, TN 37232 [BL, YM, CC, DEH].

[1]To whom reprints should be addressed:

Bo Lu, M.D., Ph.D.

Department of Radiation Oncology

Vanderbilt University

1301 22nd Avenue South, B-902 The Vanderbilt Clinic

Nashville, Tennessee 37232-5671

Telephone: (615)-343-9233

FAX: (615)-343-3075

Email: bo.lu@vanderbilt.edu

Running Title: mTOR as a therapeutic target.

Acknowledgements:

[1] Supported in part by DOD PC031161(BL), BC 030542 (BL) and a Vanderbilt Discovery Grant.

Abbreviations: HUVEC, human umbilical vein endothelial cells; VEGF, vascular endothelial growth factor; PTEN, phosphate and tensin homologue deleted on chromosome ten; PI3K, Phosphoinositol-3 kinase; mTOR, Mammalian target of rapamycin

Abstract

It is known that radiation activates the PI3K/Akt pathway and that inhibition of PI3K or Akt sensitizes tumor vasculature to radiotherapy. mTOR is a downstream target of Akt, and we hypothesized that irradiation activates mTOR signaling in both glioma and endothelial cells. By inhibiting this activation we hypothesized that we could increase radiosensitization of these cell lines. Two compounds which selectively inhibit mTOR, Rapamycin and RAD001 (everolimus) were used in this study. Both compounds caused a significant increase in sensitization of vascular endothelial cells with only minor effects on glioma cell radiosensitivity as determined by clonogenic assay. Therefore, we specifically investigated the anti-angiogenic effects of mTOR inhibitors. Increased phospho-mTOR protein was detected in irradiated HUVEC cells with no detectable increase in total mTOR protein. Phospho-S6, a biomarker for mTOR signaling, was also found to be induced following irradiation and this effect was inhibited by PI3K or mTOR inhibitors. Significant increase in cleaved caspase 3 was detected when Rad001 was combined with radiation. Endothelial tube formation was significantly diminished following treatment with Rapamycin and 3 Gy. Power Weighted Doppler of glioma xenografts in mice showed a significant reduction in vasculature and blood flow compared with mice treated with 3 Gy or RAD001 alone. We conclude that irradiation activates mTOR signaling in vascular endothelium and that Rapamycin and RAD001 increased apoptosis of endothelial cells in response to radiation. To the authors' best knowledge this is the first study which demonstrates that mTOR inhibitors may be a way to target the vasculature by radiosensitizing the vascular endothelium resulting in better tumor control as seen in experiments demonstrating increased tumor growth delay in mice treated with rapamycin with radiation compared with mice treat with either alone.

We conclude that mTOR inhibitors have increased efficacy as antiangiogenics when combined with radiation.

Introduction

Approximately 17,400 primary brain tumors are newly diagnosed each year in the United States (Landis et al., 1998). The incidence of malignant glial neoplasms account for more than 60% of primary adult brain tumors of which about 75 % are Glioblastoma Multiforme *(GBM) (Grade IV)*. Patients with GBM have median survivals of only 8 to 10 months (Curran et al., 1993). Radiation therapy remains the single most effective adjuvant treatment for malignant astrocytomas (Salazar & Rubin, 1976; Walker et al., 1980). However, most patients treated with standard radiation therapy alone have in-field recurrences that inevitably lead to the patient's death because no adequate salvage therapy exists (Hochberg & Pruitt, 1980; Wallner et al., 1989). Radiation resistance of malignant gliomas is partly due to their vascular abundance. The up-regulation of angiogenesis is a key event that accompanies glioma progression (Leon et al., 1996; Wesseling et al., 1997). Phosphoinositol-3 kinase kinase/Akt survival pathway has been found to be responsible for tumor promotion, aggressiveness, and resistance to both radiotherapy and BCNU-based chemotherapy in glioblastoma cells (Chakravarti et al., 2002; Ermoian et al., 2002; Holland et al., 2000; Sonoda et al., 2001). Inhibition of the PI3K/Akt pathway radiosensitizes tumor vasculature in mouse glioma models, possibly by inhibiting radiation-activated Akt phosphorylation in endothelial cells (Edwards et al., 2002; Tan & Hallahan, 2003). Similar Akt activation was shown to be induced by ionizing radiation in a glioma cell line via the EGFR pathway (Chakravarti et al., 2002). Therefore, blocking the pro-survival activity of PI3K/Akt that is induced by radiation may augment cytotoxic effects upon both glioma cells and its vasculature.

Mammalian target of rapamycin (**mTOR**) is a downstream target of Akt (Nave et al., 1999). It was shown that VEGF-stimulated HUVEC proliferation was effectively inhibited by Rapamycin, indicating that mTOR is a key molecule for endothelial cell

survival (Yu & Sato, 1999). mTOR may also be important for the survival of glioma cells since certain glioma cell lines were shown to be sensitive to Rapamycin and its derivatives (Hosoi et al., 1998). mTOR has also been shown to affect cells in numerous ways including decreased proliferation, increased apoptosis, and induction of autophagy, all of which appear to be cell line dependent (Huang & Houghton, 2003; Majumder et al., 2004; Munafo & Colombo, 2001). The present study examined whether mTOR signaling is activated by irradiation and whether mTOR inhibitors, Rapamycin and RAD001, could sensitizes glioma to radiotherapy by inhibiting either angiogenesis or tumor growth, and by which mechanism cell death occurs.

Experimental Procedures

Cell Culture:

HUVECs were obtained from Clonetics and were maintained in EBM-2 medium supplemented with EGM-2 MV single aliquots (BioWhittaker). GL261 cells were maintained in DMEM with Nutrient Mixture F-12 1:1 (Life Technologies, Inc.) with 7% FCS, 0.5% penicillin-streptomycin, and 1% sodium pyruvate. All cells were incubated in a 37°C in a 5% CO_2 incubator. Irradiation was given, by use of a Cobalt-60 radioactive source.

Western Immunoblots:

Cells were treated or irradiated according to the individual study (Doses: LY294002 3 μM, Rapamycin 100 nM, RAD001 50 nM). At the time of harvest, cells were counted and then washed with iced-cold PBS twice before the addition of lysis buffer (20 nM Tris, 150 mM NaCl, 1 mM EDTA, 1% Triton X-100, 2.5 mM sodium PPI, 1 mM phenylmethylsulfonyl fluoride, and leupeptin). Protein concentration was quantified by the Bio-Rad method. Equal amounts of protein were loaded into each well and separated by 10% SDS-PAGE gel, followed by transfer onto nitrocellulose membranes. Membranes were blocked by use of 10% nonfat dry milk in PBS for 2 h at room temperature. The blots were then incubated with the rabbit-anti phospho-mTOR (Ser2448), total mTOR, cleaved caspase 3, total Caspase 3, β-actin, phospho-S6, total-S6, (Cell Signaling) antibodies overnight at 4°C. Goat antirabbit IgG secondary antibody (1:1000; Amersham) was incubated for 1 h at room temperature. Immunoblots were developed by using the enhanced chemiluminescence (ECL) detection system (Amersham) according to the manufacturer's protocol and autoradiography.

In vitro Clonogenic Assay:

HUVEC and GL261 cells were treated with either rapamycin at a dose of 100 nM or DMSO for one hour. Cells were irradiated with 3 gy and media was changed. After irradiation, cells were returned to 37 °C incubation and maintained for 2 weeks. Cells were then fixed for 15 min with 3:1 methanol: acetic acid and stained for 15 min with 0.5% crystal violet (Sigma) in methanol. After staining, colonies were counted by the naked eye with a cutoff of 50 viable cells. Surviving fraction was calculated as (mean colony counts)/(cells inoculated)×(plating efficiency), where plating efficiency was defined as (mean colony counts)/(cells inoculated for un-irradiated controls). HUVEC were examined further with RAD001 at a 5 nM dose as done previously with rapamycin.

Tumor Volume Assessment

C57BL/6 mice received subcutaneous injection of one million GL261 cells into the right hind limb. After 7-10 days when average tumor volume reached 0.2 cm^3, mice were stratified into groups (five mice per group), so that the mean tumor volume in each group was comparable. Mice were then treated with rapamycin at a dose of 2 mg/kg. Treatment groups consisted of: DMSO control, Rapamycin alone, Radiotherapy alone, and Rapamycin +Radiotherapy respectively. The radiation groups received 3 Gy of radiation fractionated over 14 days (twice a week) using a Cobalt irradiator to the tumor with the remainder of the body shielded with lead. Rapamycin was administered orally at a dose of 2 mg/kg prior to radiotherapy and twice a week after the completion of radiotherapy. Tumor volume measurements began on treatment day 1 and continued twice a week until the tumor volumes became 10% of the body size. Measurements were

made using skin calipers, as previously described (Edwards et al., 2002). Tumor volumes were calculated using a formula (a x b x c/2) that was derived from the formula for an ellipsoid. Data was calculated as the percentage of the original (day 1) tumor volume and graphed as percent change in tumor volume +/- SD for each treatment group

Color Doppler Sonography

C57BL/6 mice with implanted as described in the tumor volume methods. Mice were treated with oral RAD001 at a dose of 2.5 mg/kg as described above. Tumor models in the four treatment groups underwent non-invasive color Doppler sonographic (CDS) imaging to quantitatively assess tumor blood flow, using a 10-5 MHz linear array Entos probe attached to an HDI 500 ultrasound scanner (ATL/Philips, Bothell, WA). CDS images were obtained with a power gain of 82%. Care was taken to minimize motion artifact during image acquisition. A 10-second cineloop of the entire tumor area was obtained with the transducer positioned perpendicularly to the long axis of the lower extremity. Post-processing of tumor images with HDI-lab software (ATL/Philips) allowed for the calculations of color pixel density [CPD= (# of color pixels in tumor region)/(total # of pixels in tumor region)] and mean power of color pixels [MPCP=(sum of color pixel intensities in region)/(total area of color pixels in region) for individual regions of interest. Regions of interest were manually defined for 1) the entire tumor area and 2) the superficial peripheral zone at the edge of the tumor. These measurements were acquired at two time points over the course of tumor growth to longitudinally assess changes in tumor blood flow and vascularity.

Mean values of CDP and MPCP for each of the four groups of mice before and after treatment were calculated, and the Student's unpaired t test was employed to make

statistical comparisons for vascularity before and after treatment. P values of less than 0.5 were considered significant.

Endothelial Cell (EC) Morphogenesis Assay: Tube Formation.

HUVEC cells were treated with rapamycin (100 nM), radiotherapy or both. To examine the ability of the treated HUVECs to produce tubular structures *in vitro*, 24-well plates were coated with 300 µl of Matrigel (BD Bioscience). When plated on Matrigel, the rapamycin treated or irradiated HUVECs were trypsinized and seeded at 48,000 cells/well. These cells undergo differentiation into capillary-like tube structures and were periodically observed by microscope. Tubules were stained with cell staining solution for 30 minutes at room temperature. Stained tubules were washed 3x with PBS and absorbance was read at 550 nm. Capillary-like structures were counted in triplicate using low power fields (x40), and percentage inhibition was expressed assuming untreated differentiated ECs as 100%.

Results:

mTOR inhibitor, rapamycin, sensitizes glioma and endothelial cells to radiation by decreasing cell survival:

Rapamycin is a known inhibitor of mTOR. To determine whether inhibition of mTOR is sufficient to sensitize GL261 and HUVEC cells to radiotherapy clonogenic assays were performed. Both GL261 and HUVEC were treated with either 100 nM of Rapamycin or a DMSO control and incubated for one hour. This was followed with escalating radiation doses from 0-7 Gy. The Rapamycin or DMSO was washed off after irradiation. After 2 weeks, colonies were stained and the scored colonies were graphed. This experiment was repeated in HUVEC cells treated with RAD001 at a dose of 5 nM.

Cells treated with rapamycin or Rad001 alone had reduced plating efficiency. Interestingly, rapamycin significantly lowered the survival curve of irradiated HUVEC cells but only had a minor effect on GL261 cells as shown in Figure 1A and B respectively. Similar inhibitory effects were observed when HUVEC were treated with 5 nM of Rad001 as shown in Figure 1C.

Irradiation induces mTOR signaling in endothelial cells:

In order to determine whether irradiation activates the mTOR signaling pathway in endothelial cells, HUVEC cells were irradiated with 3 Gy and phosphorylated mTOR protein levels were measured by Western immunoblots which were probed for with p-mTOR antibody at the indicated time points. As shown in Figure 2A, phosphorylated mTOR was increased at 15 minutes following 3 Gy in HUVEC. The increase in phospho-mTOR persisted at one hour after irradiation, however, the level of total mTOR protein did not increase following irradiation with 3Gy in HUVEC. We then examined the change of a biomarker for mTOR activity, phosphor-S6, following treatment with an

mTOR inhibitor and radiation. HUVEC cells were treated with LY294002 (3 μM), a known PI3K inhibitor, or Rad001 (50 nM). 30 minutes after treatment with either inhibitor, cells were treated with 3 Gy of radiation. Cell lysates were then collected and run on gels. Gels were probed for total and phospho-S6, which is downstream from mTOR and when phosphorylated serves as a biomarker for mTOR activation. As shown in Figure 2B, HUVEC treated with 3 Gy showed increased levels of S6 phosphorylation. Cells treated with LY294002 or Rad001 alone showed very little S6 phosphorylation either with or without irradiation, similar to non-irradiated HUVEC.

mTOR inhibition induces apoptosis in HUVEC:

To determine whether mTOR inhibition induces apoptosis in HUVEC we used western analysis to probe for cleaved caspase 3. HUVEC were treated with vehicle (DMSO), 3 Gy, Rad001 (50 nM) and Rad001 with 3 Gy. Cells were treated with Rad001 one hour prior to radiation and proteins were collected 6 hours later. Cleaved caspase 3 and total caspase 3 were probed for as shown in Figure 2C. DMSO alone showed no induction of caspase 3 cleavage, whereas there was minor induction of caspase 3 cleavage in cells treated with 3 Gy or Rad001 alone. However, combined therapy with Rad001 and 3 Gy resulted in the greatest increase in Caspase 3 cleavage when compared with the other groups. Total caspase 3 showed no change in all groups.

Rapamycin sensitizes vascular endothelium to radiation injury in in vitro and in vivo studies:

Since rapamycin reduced the survival of HUVEC cells, we studied rapamycin effects on tumor angiogenesis. HUVEC cells were treated with either 100 nM rapamycin or DMSO for one hour. Cells were then irradiated with 0 or 3Gy. Rapamycin and

DMSO were washed off after irradiation. The endothelial cell morphogenesis assay was performed to examine the ability of the treated HUVECs to produce tubular structures *in vitro*. As shown in Figure 3, HUVEC cells that were treated with both rapamycin and 3 Gy formed 3-4 fold less tubular structures, in contrast to the DMSO group. The groups treated with radiotherapy or rapamycin alone had nearly a one fold reduction of tubular structure.

Color Doppler Sonography (CDS) was used to determine the in vivo effects of these various treatment regimens on tumor neovascularization over the course of treatment. At the onset of treatment, all tumors in the respective groups showed a moderate amount of vascularity, as indicated by the representative image of a control tumor at the onset of treatment (Figure 4). After 11 days of tumor progression, control tumors displayed a significant increase in CDS signal. This signal was increased with respect to the tumor volume. The tumor volume is defined, and the number of color pixels within the tumor are compared to the non colored pixels in the tumor volume. Tumors receiving radiation therapy alone demonstrated a lesser increase in CDS, whereas tumors receiving systemic RAD001 at a dose of 2.5 mg/kg alone exhibited little change in CDS. Tumors receiving concomitant radiation and RAD001 demonstrated an appreciable diminution in CDS signal over the course of treatment. Because these are just subjective pictures we then used software to analyze vascularity and blood flow.

The quantified calculations of color pixel density (CPD) and mean power of color pixels (MPCP) for each group of mice are graphed in Figure 4. They were consistent with the increases and decreases subjectively ascertained from the sonographic images. CPD is an indicator of in vivo tumor vascular density whereas MPCP is more indicative of blood flow through the tumor. In the tumor peripheral zones, the subjects that received no treatments demonstrated a 95% overall increase in CPD ($P<0.001$) and a 48%

increase in MPCP ($P<0.03$). For the mice that received radiation therapy alone, tumors demonstrated relatively less vascular growth than those of the control mice, with increases of 31% for CDP and 17% for MPCP. Tumors receiving Rad001demonstrated even more restricted neovascularization and only small changes in these calculations, namely an 8% decrease in CDP and a 1% increase in MPCP. The group of mice receiving combination therapy were the only treatment group to express significant decreases in blood supply, with a 32% reduction in CDP ($P<0.05$) and 36% reduction in MPCP ($P<0.03$).

Rapamycin enhanced radiation-induced tumor regression:

To determine whether inhibition of mTOR enhances radiation-induced tumor volume regression, GL261 glioma xenograft were established and tumor volumes were measured by use of calipers, as described previously (Edwards et al., 2002). GL261 tumor-bearing mice were treated with 3 Gy twice a week for two weeks. Rapamycin was given orally at a dose of 2 mg/kg prior to radiotherapy. As shown in Figure 5 a and b, the prescribed doses of radiotherapy or rapamycin were effective in controlling the growth of GL261 xenografts. Rapamycin given with radiation induced tumor growth delays of 18 days and 15 days, respectively, when compared with radiation alone.

Discussion:

Akt activation is known to be induced by irradiation in both glioma and endothelial cells and is upstream of mTOR. In the present study, we have shown that irradiation activates mTOR signaling in vascular endothelium, and that this activation is mediated by PI3K, however there was minimal radiosensitization on GL261 cells. Based on these findings we investigated the effects of mTOR inhibition on HUVEC cells. We found that levels of phospho-mTOR and Phospho-S6 are increased following irradiation in HUVEC.

mTOR is becoming an important target for a new line of anti-cancer drugs such as CCI-779 and RAD001, which are derived from rapamycin and exhibit significant anti-cancer activity in various tumor cell lines (Boulay et al., 2004; Huang & Houghton, 2003). The activation of mTOR enhances protein translation via phosphorylating eukaryotic initiation factor 4E-binding protein 1 (4E-BP1) and 70-kDa S6 kinase (S6K1) (Raught et al., 2001). S6 phosphorylation has been used as a biomarker for mTOR activation (Eshleman et al., 2002). mTOR may be essential for the survival of glioma since certain glioma cell lines were shown to be sensitive to rapamycin and its derivatives (Hosoi et al., 1998). Furthermore, rapamycin has been reported to sensitize U87 glioma xenografts to radiotherapy (Eshleman et al., 2002). Consistent with our results, Eshelman et al. also found that a monolayer of glioma cells treated with Rapamycin had no change in radiosensitivity. This study also showed that when glioma cells were grown in spheroids, treatment with rapamycin induced radiosensitization and the authors purpose that this effect may be due to rapamycin improving the oxygenation of the spheroids. This study demonstrated that there is a radiosensitizing effect intrinsic to the tumor mass that is independent of the host component (Eshleman et al., 2002). However, they also

postulated that the host component was important in the improved tumor growth delay observed in animals treated with rapamycin and radiation (Eshleman et al., 2002).

In our study, we addressed the role of the host component of glioma and more specifically the effects of rapamycin on the radiosensitivity of gliomal vasculature. We found that rapamycin failed to induce radiosensitization in GL261 monolayers, in agreement with Eshleman et al (Eshleman et al., 2002). In contrast, the radiosensitizing effect of mTOR inhibition on HUVEC monolayers was shown in colony assays. Further evidence that mTOR inhibition is an effective vascular radiosensitizer are found in previous studies that have shown that rapamycin inhibits angiogenesis, likely by reducing VEGF expression (Guba et al., 2002). Geng et al have shown that VEGF inhibition has a radiosensitizing effects on tumor vasculature (Geng et al., 2001). Further studies have suggested that reduced VEGF expression may induce its antiangiogenic effects in a S6 dependent fashion (Yu & Sato, 1999). These findings suggest that in addition to the direct effects of rapamycin on tumor cells in in vivo models, rapamycin is also causing an antiangiogenic effect.

To the authors' knowledge, this is the first study to demonstrate the radiosensitizing effects of rapamycin on the host vasculature. Results from in vitro endothelial cell tubule formation assays suggest that mTOR inhibition augments the effects of radiation on vascular endothelial migratory ability. These results indicated that rapamycin had significant inhibitory effects on tubule formation, consistent with rapamycin's antiangiogenic effects shown in by Guba et al (Guba et al., 2002). Doppler data further supports this with in vivo data. Results indicated significant reduction in vascularity and flow of tumors treated with mTOR inhibitors alone, also consistent with Guba et al (Guba et al., 2002). We have shown that radiation used in combination with mTOR inhibitors had an even greater effect on the tumor vasculature when compared

with either treatment alone. From these results, we purpose that mTOR inhibitors are an important radiosensitizer in the vascular endothelium. Tumor volume study results in mice further supposr this, with a significant increase in growth delay in mice treated with rapamycin and radiation compared with either treatment alone, consistent with the findings of Eshleman et al.

The difference between GL261 and HUVEC response to radiation given with mTOR inhibitors has several explanations. Several different mutations and differences in protein expression have been found to be linked to how cells respond to mTOR inhibition (Huang & Houghton, 2001). Malignant cell lines show a remarkable variance in sensitivity to rapamycin, displaying a several thousand-fold difference in intrinsic sensitivity (Dilling et al., 1994). However, the vascular endothelium provides a consistent target across both different cell lines and the heterogenicity within a cancer type. Furthermore, whether rapamycin induces a cytotoxic, cytostatic, or a cytotoxic/cytostatic response appears to be cell line dependent (Hosoi et al., 1998; Hosoi et al., 1999; Huang et al., 2001). ATM (Beamish et al., 1996), p53 (Huang et al., 2001) and PTEN (Majumder et al., 2004), have all been linked to rapamycin resistance. PTEN is mutated in 20-30% of glioblastoma (Duerr et al., 1998; Li et al., 1997). Low expression levels of PTEN were associated with poor patient survival, possibly by up-regulating Akt (Ermoian et al., 2002). PTEN gene transfer results in inhibition of S-phase entry in glioblastoma cells (Cheney et al., 1999), reduced growth and angiogenesis in mouse glioma models (Wen et al., 2001) and sensitization to irradiation in glioma cell cultures (Wick et al., 1999). P53 mutations are the most common abnormality in human malignancy (Gaidano et al., 1991) and p53 is mutated in approximately one third of gliomas (Lang et al., 1994; Newcomb et al., 1993).

Additional defects that may lead to resistance in certain cell lines include defects in FKBP12 and the FRB domain. To bind to the FRB domain and inhibit mTOR, rapamycin must first bind to FKBP12. Mutations in either the FKBP12 protein (Dumont et al., 1995) or the FRB domain (Chen et al., 1995; Dumont et al., 1995) attenuate Rapamycin binding ability. Downstream targets of mTOR may also be mutated or have a decrease in production leading to rapamycin resistance. S6K1 is a major downstream target of mTOR and several mutation in S6K1 phosphorylation sites are associated with resistance to rapamycin (Dennis et al., 1996). Another protein, 4E-BP1, a suppressor of eIF4E, is also known to be a downstream target of mTOR (Gingras et al., 2001). Recently it has been shown that decreased levels of 4E-BP1 are also associated with rapamycin resistance (Dilling et al., 2002). Differences in these proteins may also explain the different response between GL261 and HUVEC cells. It also provides a rational for focusing on the vascular endothelium for radiosensitization due to less heterogeneity across patients.

In summary, our data suggests that irradiation activates mTOR cell survival signaling in glioma vascular endothelium via a PI3K/Akt dependent pathway. mTOR inhibition resulted in marked increase in HUVEC radiosensitization with only minor sensitization in GL261 cells. Rapamycin's effects on vascular endothelium were further confirmed with tubule formation studies and Power Doppler studies which indicated that vascular endothelium was affected in both in vitro and in vivo. We demonstrated that RAD001 is an effective radiosensitizer in the GL261 glioma model using tumor volume curves.

Figure Legends:

Figure 1. mTOR inhibition radiosensitizes HUVEC but not GL261 cells. GL261 and HUVEC cells were treated with 100 nM of rapamycin or DMSO for one hour. Cells were then irradiated with 3 Gy and media was changed. After two weeks colonies were scored. Shown are GL261 (A) and HUVEC (B) treated with radiation alone and radiation with rapamycin at indicated doses. RAD001 (50 nM) treated HUVEC are shown in C.

Figure 2. Radiation induces mTOR phosphorylation in HUVEC: HUVEC cells were treated with 3 Gy and cell lysates were collected at 0, 15, 30, 60 minutes. Shown are HUVEC lysates run on a gel treated with p-mTOR and m-TOR antibodies (A). To determine whether mTOR activation was PI3K dependent a PI3K inhibitor, LY294002 was used. mTOR activation was confirmed by probing for S6 phosphorylation, a biomarker for mTOR activation. HUVEC were treated with DMSO, 3 Gy, LY294002 (3 μM), Rad001 (50 nM), LY294002 with 3 Gy, and Rad001 with 3 Gy. Shown are western blot probed for phosphorylated S6 and total S6 (B). HUVEC were treated with DMSO, 3 Gy, Rad001 (50nM) or Rad001 with 3 Gy. Shown are western blots probed for cleaved caspase 3 and total caspase 3 (C).

Figure 3. Rapamycin sensitizes vascular endothelium to radiation injury: HUVEC (4.8×10^4 cells) were treated with rapamycin (100 nM), radiation, or both. They were then resuspended and plated on 24-well plates coated with Matrigel, as described in the "Materials and Methods" section. After 24 hours, the media were gently aspirated and the cells were fixed and stained. The slides were examined for tube formation by microscopy

(x 40). Representative figures and quantitation of tubular structures are shown. Data is shown as the mean +/- SD.

Figure 4. Longitudinal changes in tumor blood supply in various treatment conditions: Color Doppler ultrasound images depict longitudinal development of blood supply in in vivo murine GL261 tumors (4A) before treatment. After 11 days of treatment mice tumors were redopplered. Shown are (4B) no treatment intervention, (4C) radiation treatment alone, (4D) systemic RAD001 (2.5 mg/kg) chemotherapy, and (4E) concomitant irradiation and RAD001. Tumors borders are visible as oval masses surrounded by normal muscle. Color Doppler signal indicates relative blood flow, with the biggest increases neovascularity occuring in untreated tumors, and marked diminution of vascularity in tumors receiving combined irradiation and RAD001.

Color Doppler sonographic calculations of percent changes of color density of pixels (CDS), which correlates with tumor vascularity, and mean power of color pixels (MPCP), which correlates with tumor blood flow as shown in figure 4 (bottom). Control tumors demonstrated significant increases in vascularity and blood flow, whereas tumors receiving combination RAD001 with radiation demonstrated significant decreases in blood flow. (* $P < 0.001$; ** $P < 0.05$, † $P < 0.03$).

Figure 5. Rapamycin enhanced radiation-induced tumor regression: GL261 tumors implanted in the hind limb of C57BL/6 mice (five mice per treatment group) were treated with 2 mg/kg of rapamycin (p.o.), with or without 3 Gy twice a week for two weeks. Fold increase in tumor volume was calculated as the ratio of current volume divided by original tumor volume (day 1) (V/V_i) and graphed (A) as fold change in tumor volume +/- SD for each treatment group.

Beamish, H., Williams, R., Chen, P., Khanna, K.K., Hobson, K., Watters, D., Shiloh, Y. & Lavin, M. (1996). *Oncogene*, **13,** 963-70.

Boulay, A., Zumstein-Mecker, S., Stephan, C., Beuvink, I., Zilbermann, F., Haller, R., Tobler, S., Heusser, C., O'Reilly, T., Stolz, B., Marti, A., Thomas, G. & Lane, H.A. (2004). *Cancer Res*, **64,** 252-61.

Chakravarti, A., Chakladar, A., Delaney, M.A., Latham, D.E. & Loeffler, J.S. (2002). *Cancer Res*, **62,** 4307-15.

Chen, J., Zheng, X.F., Brown, E.J. & Schreiber, S.L. (1995). *Proc Natl Acad Sci U S A*, **92,** 4947-51.

Cheney, I.W., Neuteboom, S.T., Vaillancourt, M.T., Ramachandra, M. & Bookstein, R. (1999). *Cancer Res*, **59,** 2318-23.

Curran, W.J., Jr., Scott, C.B., Horton, J., Nelson, J.S., Weinstein, A.S., Fischbach, A.J., Chang, C.H., Rotman, M., Asbell, S.O., Krisch, R.E. & et al. (1993). *J Natl Cancer Inst*, **85,** 704-10.

Dennis, P.B., Pullen, N., Kozma, S.C. & Thomas, G. (1996). *Mol Cell Biol*, **16,** 6242-51.

Dilling, M.B., Dias, P., Shapiro, D.N., Germain, G.S., Johnson, R.K. & Houghton, P.J. (1994). *Cancer Res*, **54,** 903-7.

Dilling, M.B., Germain, G.S., Dudkin, L., Jayaraman, A.L., Zhang, X., Harwood, F.C. & Houghton, P.J. (2002). *J Biol Chem*, **277,** 13907-17.

Duerr, E.M., Rollbrocker, B., Hayashi, Y., Peters, N., Meyer-Puttlitz, B., Louis, D.N., Schramm, J., Wiestler, O.D., Parsons, R., Eng, C. & von Deimling, A. (1998). *Oncogene*, **16,** 2259-64.

Dumont, F.J., Staruch, M.J., Grammer, T., Blenis, J., Kastner, C.A. & Rupprecht, K.M. (1995). *Cell Immunol*, **163,** 70-9.

Edwards, E., Geng, L., Tan, J., Onishko, H., Donnelly, E. & Hallahan, D.E. (2002). *Cancer Res*, **62,** 4671-7.

Ermoian, R.P., Furniss, C.S., Lamborn, K.R., Basila, D., Berger, M.S., Gottschalk, A.R., Nicholas, M.K., Stokoe, D. & Haas-Kogan, D.A. (2002). *Clin Cancer Res*, **8,** 1100-6.

Eshleman, J.S., Carlson, B.L., Mladek, A.C., Kastner, B.D., Shide, K.L. & Sarkaria, J.N. (2002). *Cancer Res*, **62,** 7291-7.

Gaidano, G., Ballerini, P., Gong, J.Z., Inghirami, G., Neri, A., Newcomb, E.W., Magrath, I.T., Knowles, D.M. & Dalla-Favera, R. (1991). *Proc Natl Acad Sci U S A*, **88,** 5413-7.

Geng, L., Donnelly, E., McMahon, G., Lin, P.C., Sierra-Rivera, E., Oshinka, H. & Hallahan, D.E. (2001). *Cancer Res*, **61,** 2413-9.

Gingras, A.C., Raught, B. & Sonenberg, N. (2001). *Genes Dev*, **15,** 807-26.

Guba, M., von Breitenbuch, P., Steinbauer, M., Koehl, G., Flegel, S., Hornung, M., Bruns, C.J., Zuelke, C., Farkas, S., Anthuber, M., Jauch, K.W. & Geissler, E.K. (2002). *Nat Med*, **8,** 128-35.

Hochberg, F.H. & Pruitt, A. (1980). *Neurology*, **30,** 907-11.

Holland, E.C., Celestino, J., Dai, C., Schaefer, L., Sawaya, R.E. & Fuller, G.N. (2000). *Nat Genet*, **25,** 55-7.

Hosoi, H., Dilling, M.B., Liu, L.N., Danks, M.K., Shikata, T., Sekulic, A., Abraham, R.T., Lawrence, J.C., Jr. & Houghton, P.J. (1998). *Mol Pharmacol*, **54,** 815-24.

Hosoi, H., Dilling, M.B., Shikata, T., Liu, L.N., Shu, L., Ashmun, R.A., Germain, G.S., Abraham, R.T. & Houghton, P.J. (1999). *Cancer Res*, **59,** 886-94.

Huang, S. & Houghton, P.J. (2001). *Drug Resist Updat*, **4,** 378-91.

Huang, S. & Houghton, P.J. (2003). *Curr Opin Pharmacol*, **3,** 371-7.

Huang, S., Liu, L.N., Hosoi, H., Dilling, M.B., Shikata, T. & Houghton, P.J. (2001). *Cancer Res*, **61,** 3373-81.

Landis, S.H., Murray, T., Bolden, S. & Wingo, P.A. (1998). *CA Cancer J Clin*, **48,** 6-29.

Lang, F.F., Miller, D.C., Koslow, M. & Newcomb, E.W. (1994). *J Neurosurg*, **81,** 427-36.

Leon, S.P., Folkerth, R.D. & Black, P.M. (1996). *Cancer*, **77,** 362-72.

Li, J., Yen, C., Liaw, D., Podsypanina, K., Bose, S., Wang, S.I., Puc, J., Miliaresis, C., Rodgers, L., McCombie, R., Bigner, S.H., Giovanella, B.C., Ittmann, M., Tycko, B., Hibshoosh, H., Wigler, M.H. & Parsons, R. (1997). *Science*, **275,** 1943-7.

Majumder, P.K., Febbo, P.G., Bikoff, R., Berger, R., Xue, Q., McMahon, L.M., Manola, J., Brugarolas, J., McDonnell, T.J., Golub, T.R., Loda, M., Lane, H.A. & Sellers, W.R. (2004). *Nat Med*, **10,** 594-601.

Munafo, D.B. & Colombo, M.I. (2001). *J Cell Sci*, **114,** 3619-29.

Nave, B.T., Ouwens, M., Withers, D.J., Alessi, D.R. & Shepherd, P.R. (1999). *Biochem J*, **344 Pt 2,** 427-31.

Newcomb, E.W., Madonia, W.J., Pisharody, S., Lang, F.F., Koslow, M. & Miller, D.C. (1993). *Brain Pathol*, **3,** 229-35.

Raught, B., Gingras, A.C. & Sonenberg, N. (2001). *Proc Natl Acad Sci U S A*, **98,** 7037-44.

Salazar, O.M. & Rubin, P. (1976). *Int J Radiat Oncol Biol Phys*, **1,** 627-37.

Sonoda, Y., Ozawa, T., Aldape, K.D., Deen, D.F., Berger, M.S. & Pieper, R.O. (2001). *Cancer Res*, **61,** 6674-8.
Tan, J. & Hallahan, D.E. (2003). *Cancer Res*, **63,** 7663-7.
Walker, M.D., Green, S.B., Byar, D.P., Alexander, E., Jr., Batzdorf, U., Brooks, W.H., Hunt, W.E., MacCarty, C.S., Mahaley, M.S., Jr., Mealey, J., Jr., Owens, G., Ransohoff, J., 2nd, Robertson, J.T., Shapiro, W.R., Smith, K.R., Jr., Wilson, C.B. & Strike, T.A. (1980). *N Engl J Med*, **303,** 1323-9.
Wallner, K.E., Galicich, J.H., Krol, G., Arbit, E. & Malkin, M.G. (1989). *Int J Radiat Oncol Biol Phys*, **16,** 1405-9.
Wen, S., Stolarov, J., Myers, M.P., Su, J.D., Wigler, M.H., Tonks, N.K. & Durden, D.L. (2001). *Proc Natl Acad Sci U S A*, **98,** 4622-7.
Wesseling, P., Ruiter, D.J. & Burger, P.C. (1997). *J Neurooncol*, **32,** 253-65.
Wick, W., Furnari, F.B., Naumann, U., Cavenee, W.K. & Weller, M. (1999). *Oncogene*, **18,** 3936-43.
Yu, Y. & Sato, J.D. (1999). *J Cell Physiol*, **178,** 235-46.

Figure 1.

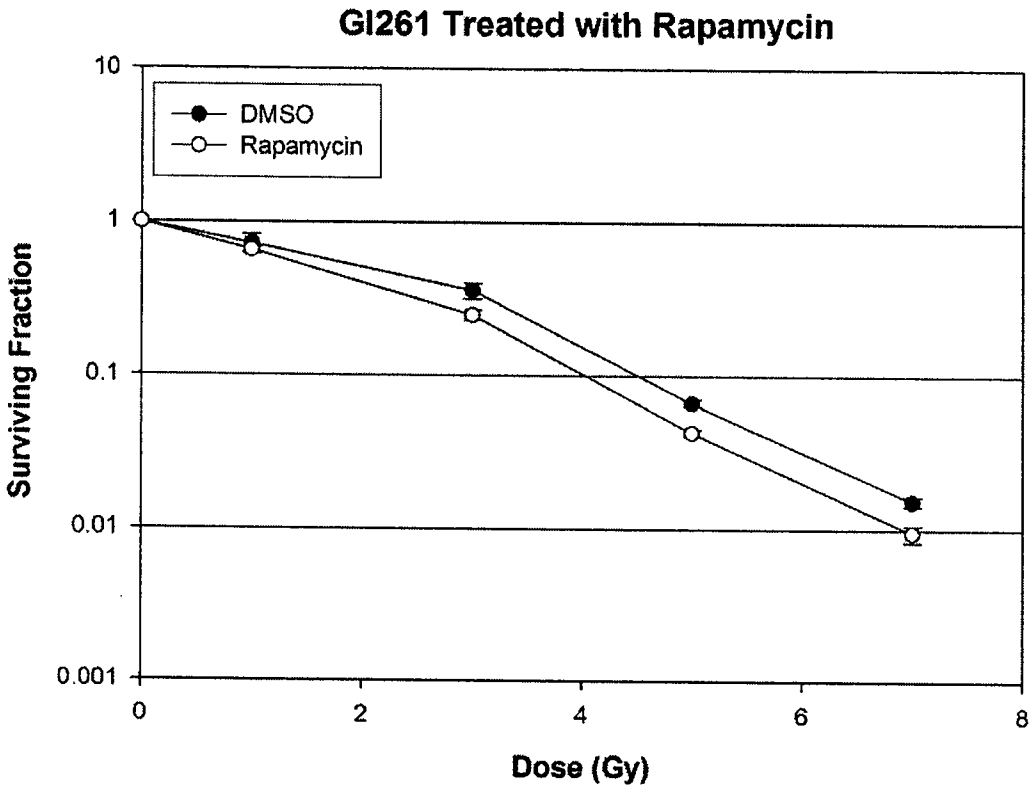
GI261 Treated with Rapamycin
DMSO
Rapamycin
Surviving Fraction
10
1
0.1
0.01
0.001
0
2
4
6
8
Dose (Gy)

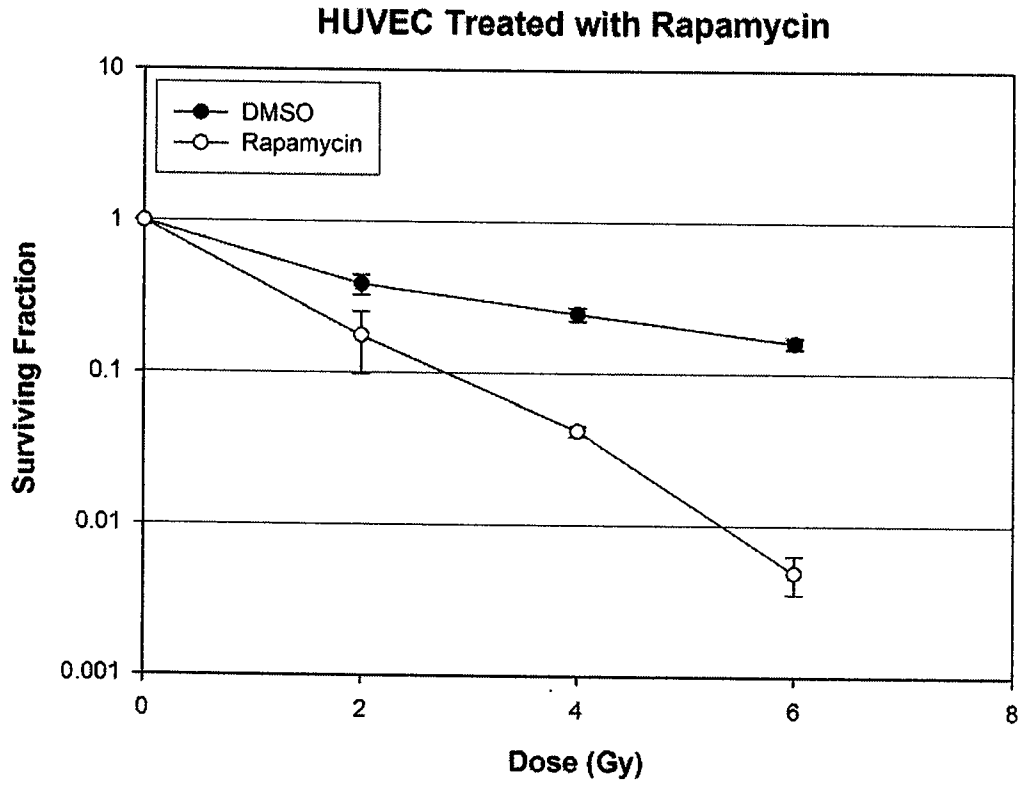
HUVEC Treated with Rapamycin
DMSO
Rapamycin
Surviving Fraction
10
1
0.1
0.01
0.001
0
2
4
6
8
Dose (Gy)

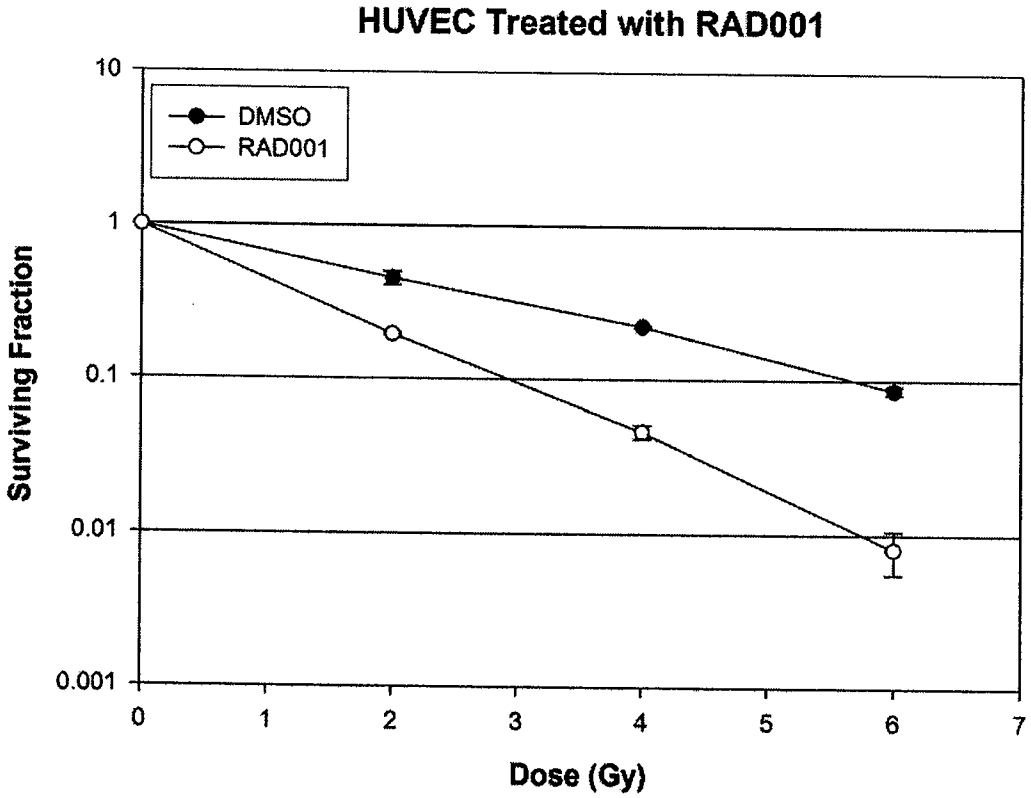
HUVEC Treated with RAD001
DMSO
RAD001
Surviving Fraction
10
1
0.1
0.01
0.001
0
1
2
3
4
5
6
7
Dose (Gy)

Figure 2.

A)

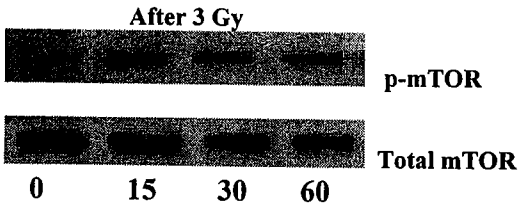
After 3 Gy
p-mTOR
Total mTOR
0
15
30
60

B)

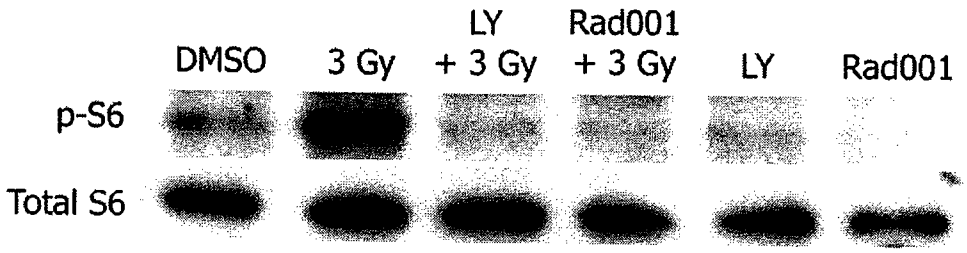
DMSO
3 Gy
LY + 3 Gy
Rad001 + 3 Gy
LY
Rad001
p-S6
Total S6

C)

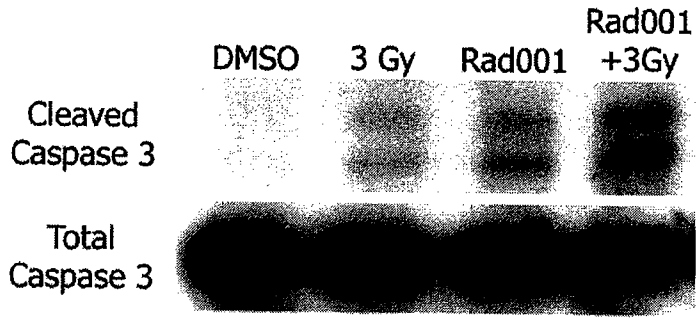
DMSO
3 Gy
Rad001
Rad001 +3Gy
Cleaved Caspase 3
Total Caspase 3

Figure 3.

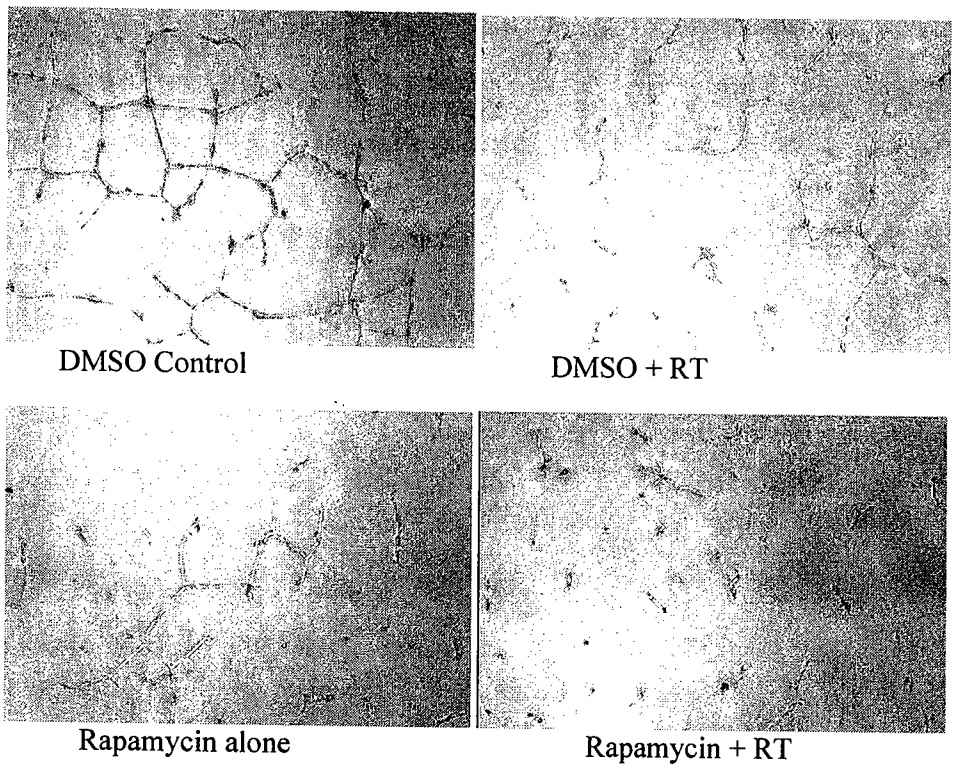

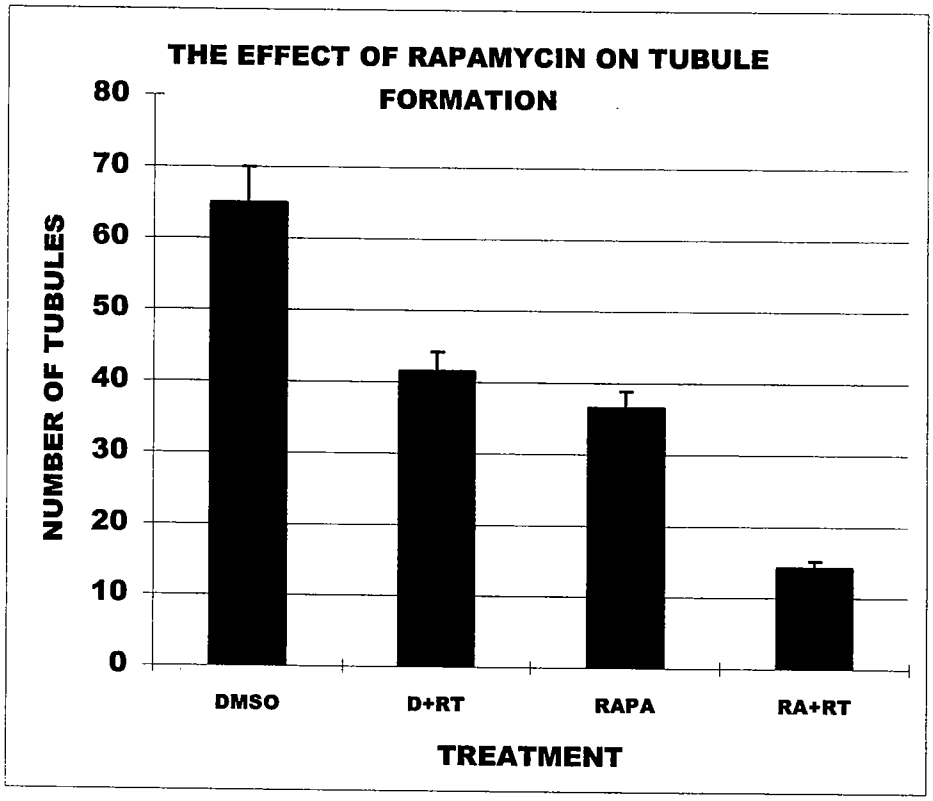
THE EFFECT OF RAPAMYCIN ON TUBULE FORMATION
NUMBER OF TUBULES
80
70
60
50
40
30
20
10
0
DMSO
D+RT
RAPA
RA+RT
TREATMENT

Figure 4.

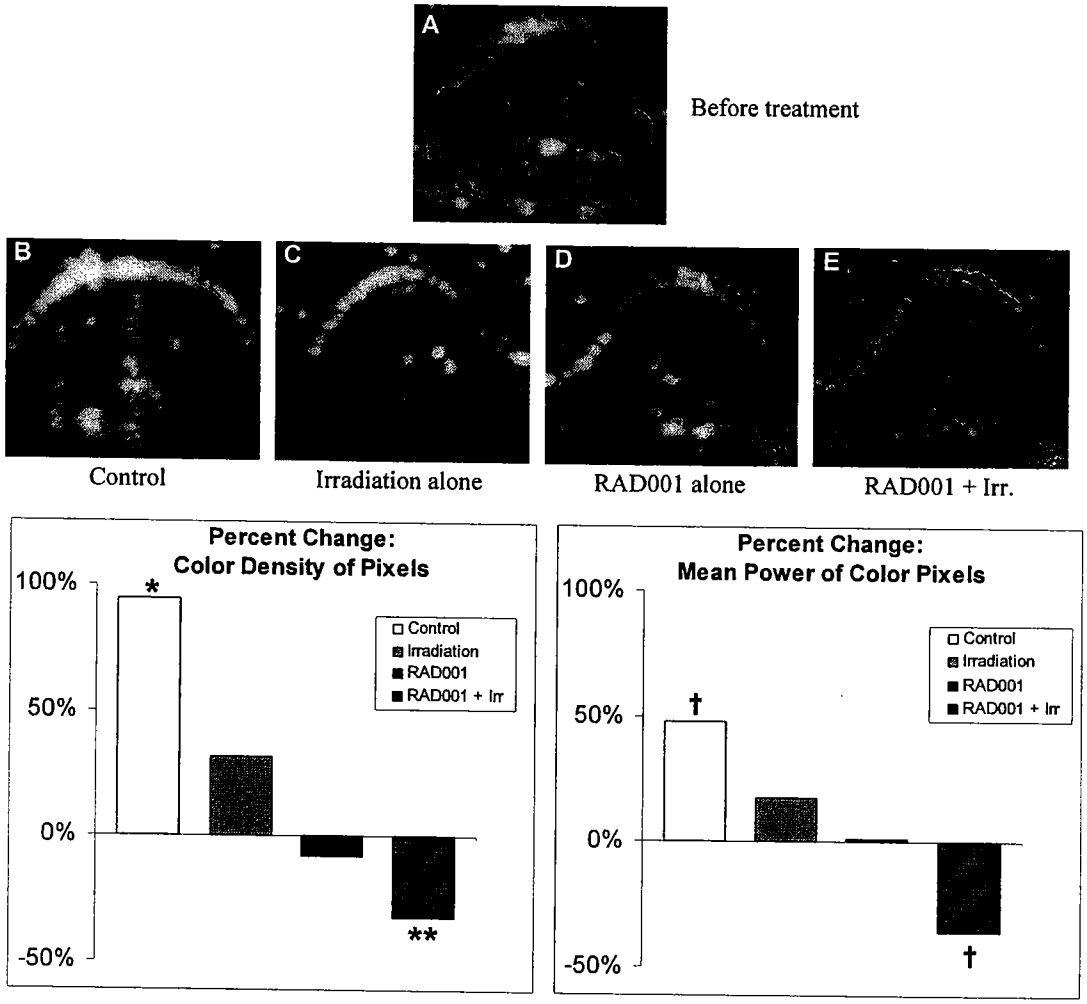
A
Before treatment
B
C
D
E
Control
Irradiation alone
RAD001 alone
RAD001 + Irr.
Percent Change:
Color Density of Pixels
100%
50%
0%
-50%
*
**
Control
Irradiation
RAD001
RAD001 + Irr
Percent Change:
Mean Power of Color Pixels
100%
50%
0%
-50%
†
†
Control
Irradiation
RAD001
RAD001 + Irr

Figure 5.

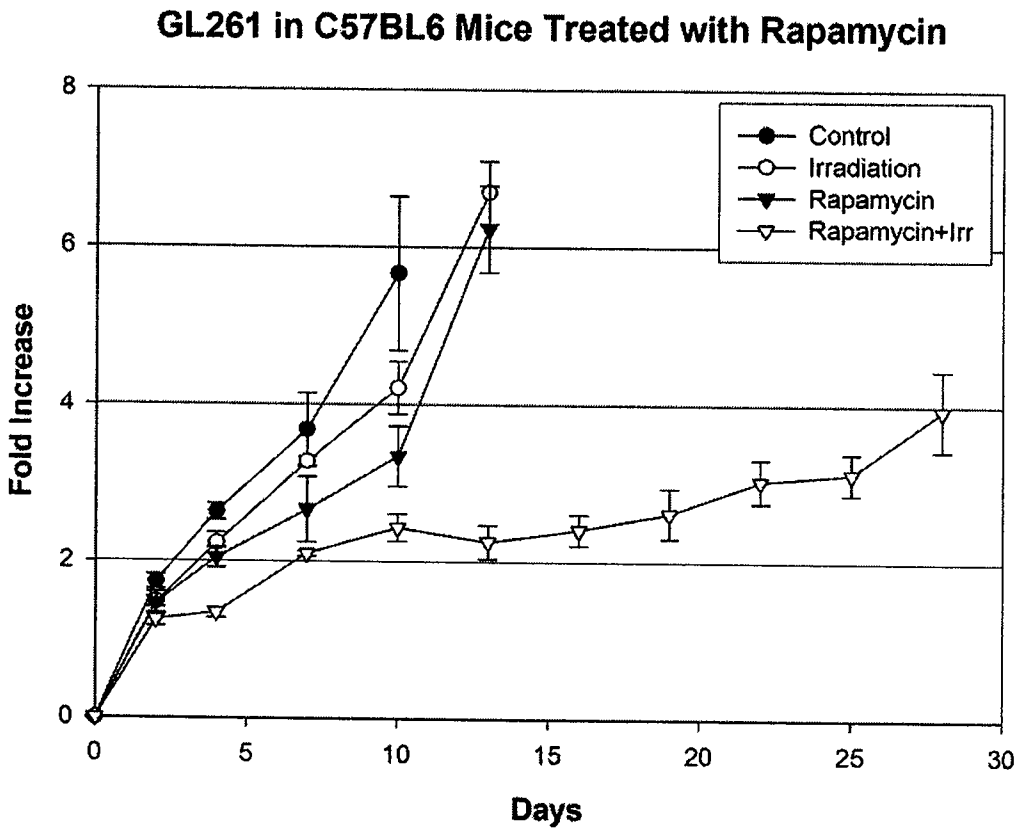
GL261 in C57BL6 Mice Treated with Rapamycin
Control
Irradiation
Rapamycin
Rapamycin+Irr
Fold Increase
Days
0
2
4
6
8
0
5
10
15
20
25
30